Hindawi
Geofluids
Volume 2023, Article ID 3819799, 23 pages
https://doi.org/10.1155/2023/3819799

Research Article

Mechanical Properties of High-Temperature Granite under Liquid Nitrogen Cooling

Linchao Wang,[1] Yi Xue,[1] Zhengzheng Cao,[2] Xiao-juan Wu,[1] Fa-ning Dang,[1] and Ruifu Liu[3]

[1]*School of Civil Engineering and Architecture, Xi'an University of Technology, Xi'an 710048, China*
[2]*Henan Key Laboratory of Underground Engineering and Disaster Prevention, Henan Polytechnic University, Jiaozuo 454000, China*
[3]*Structural and Fire Safety Engineering, School of Engineering, The University of Edinburgh, Edinburgh EH9 3JL, UK*

Correspondence should be addressed to Zhengzheng Cao; caozz@hpu.edu.cn

Received 7 November 2022; Revised 11 December 2022; Accepted 18 March 2023; Published 14 April 2023

Academic Editor: Peng Tan

The cooling characteristics of liquid nitrogen can effectively weaken the mechanical properties of dry hot rock reservoirs, improve the porosity and permeability of dry hot rock, and thus improve the development and utilization of geothermal resources. In order to explore the weakening effect of liquid nitrogen cooling characteristics on high-temperature reservoir rocks, uniaxial compression tests, Brazil splitting tests, and three-point bending tests were conducted on high-temperature granite, and synchronous acoustic emission tests were conducted to monitor the damage evolution of rocks. It is found that under the action of liquid nitrogen, the elastic modulus, peak strength, fracture toughness, and other mechanical properties of granite decrease to varying degrees. At different initial temperatures, the damage degree of liquid nitrogen to granite is different. The higher the initial temperature of granite, the greater the damage effect of liquid nitrogen on granite. The low-temperature characteristics of liquid nitrogen not only have the effect of cracking damage on granite but also have the effect of thermal stress on granite. If the temperature difference between the two is large, the heat released in the combination process will be higher. The greater the temperature difference, the greater the damage to granite. Under the action of liquid nitrogen, the acoustic emission characteristics of granite also show different evolution laws, and the ringing count of rock increases significantly, which indicates that liquid nitrogen aggravates the internal damage of granite, making the rock more fractured during fracturing. The research results can provide some scientific guidance for the development and utilization of geothermal energy.

1. Introduction

With the continuous progress of science and technology in China, people's living standards are also improving, which means that China's energy consumption is also expanding. In the face of the international environment of shortage of oil and coal resources, China must develop a new energy that is easy to use for future use. Under the exploration of people, a new type of energy—dry hot rock—has emerged in front of us. Dry hot rock is a kind of dense and impermeable high-temperature rock mass, which has a huge stock in China. Therefore, its research and development are in line with China's energy development strategy [1–3] In order to avoid energy crisis, it is very important to increase the development and utilization of new energy. China has huge reserves of dry hot rock resources, which is an important target for China's energy development direction [4–6]. The enhanced geothermal system is a new progress made in the field of geothermal energy exploitation in deep strata and other related fields in recent years [7–9]. It is a key engineering technology for extracting geothermal energy from deep strata. The main way to develop dry hot rock resources is to use the pressure of high-pressure water to make it produce many cracks. Since there are a few natural joints in dry hot rocks, the high pressure of water is used to expand them into larger cracks. Water enters the dry hot rocks and absorbs the heat energy of the dry hot rocks to raise the temperature. Recycling water is equivalent to exploiting the heat energy of the dry hot rocks [10, 11]. However, the reservoir characteristics of dry hot rock are generally low porosity, low permeability, being dense, and being deep buried. It is difficult to obtain high-temperature resources due to mining difficulties. Therefore, it is necessary to open the channel of dry hot rock and form an effective hydraulic connection to improve the heat transfer efficiency [12–14]. Therefore, how to effectively crack the dry hot rock reservoir to establish a flow channel is one of the key issues facing the development of dry hot rock.

As a new type of anhydrous fracturing technology, liquid nitrogen can be used in the process of developing and collecting dry hot rock. The chemical property of liquid nitrogen is not active, and it generally does not react with the outside world. It is an inert liquid. Using liquid nitrogen instead of water as fracturing fluid, when dry hot rock contacts with liquid nitrogen, in addition to the pressure of liquid nitrogen itself, due to the huge temperature difference between the two, a certain temperature stress will be generated, which will lead to larger and more thermally induced cracks in dry hot rock. Li et al. [15] discussed the possibility of using liquid nitrogen as fracturing fluid. Tran et al. [16] found that in the process of rock fracturing, if low-temperature fluid flows in the main fractures, fractures will be generated on the basis of the original fractures. This law will be more obvious and reflected in the natural cracks in the rock. Cai et al. [17] explored the speed of sound wave propagation in the rock and the law of permeability change of the rock under low temperature. They found through research that liquid nitrogen can cause the rock to cool down and crack, and at the same time, liquid nitrogen will gasify in the rock, which will produce gasification expansion and lead to rock fracture [18]. In this gasified liquid nitrogen plus liquid nitrogen fracturing technology, taking their advantages and disadvantages into account, they put forward the technical idea of fracturing rocks in sections by spraying liquid nitrogen and analyzed the feasibility of this technology in engineering. Therefore, studying the weakening impact of liquid nitrogen on rock mechanical properties has great potential help for the development of geothermal resources. Huang et al. [19] studied the fracture damage characteristics of rocks at low temperature. The results show that the low-temperature liquid nitrogen fracturing can cause the growth of rock microcracks and micropores, causing greater damage to rocks. At present, there are also studies on other fracturing methods, such as hydraulic fracturing, which will not be efficient and will bring about environmental pollution [20, 21].

At the end of the last century, McDaniel et al. [22] carried out liquid nitrogen cold immersion experiments on rocks. They found that if rocks were in a low-temperature liquid nitrogen environment, the rocks would shrink, deform, and break into blocks. At low temperature, a group of orthogonal cracks will be generated on the exposed surface of the fluid. If the rock is soaked repeatedly, the rock will continue to fracture. Wang et al. [23] studied the development of pore structure of rocks injected with liquid nitrogen by means of rock permeability test. They used a mercury intrusion method and concluded that the permeability of the rock injected with liquid nitrogen was significantly improved compared with the rock without liquid nitrogen injection. Cha et al. [24] studied the cold fracture of rock in combination with an acoustic emission testing method. Zhang et al. [25] conducted liquid nitrogen immersion tests on rock samples, and they concluded that liquid nitrogen will cause temperature stress and other stress concentration in the rock. Ren et al. [26] concluded that the rock matrix will be affected under the low-temperature effect of liquid nitrogen. The cracks caused by the impact stress of cold liquid nitrogen will develop along the direction perpendicular to the fracture. Due to the continuous extension of the fracture, it is helpful to increase the overall permeability of the rock. Wang et al. [27] found that liquid nitrogen immersion experiments on rocks were performed on macroscopic domains and such macroscopic observations have major drawbacks and cannot reveal the nature of the action of liquid nitrogen on rocks. Dusseault et al. [28, 29] found that when the liquid with low temperature enters the bottom of the well, the rock around the well will undergo shear failure and tensile failure. Wu et al. [30, 31] concluded that the main reason for the damage of low-temperature liquid nitrogen to rocks is that liquid nitrogen will cause damage to rocks, resulting in microcracks. Then, microcracks will extend and develop, plus the generation of new microcracks, which will damage rocks. They also pointed out that the low temperature will reduce the cracking pressure of the surface layer and deepen the crisscross degree of fractures. Hou et al. [32] found that low temperature would cause great damage to the structure and micro pores of coal. Du et al. [33] studied the damage effect of liquid nitrogen on coal and found that the damage degree of coal is different with different bedding angles. Su et al. [34] studied the damage effect of liquid nitrogen on marble and believed that the higher the initial temperature of rock, the greater the damage effect on rock. However, the current research often adopts a single experimental method and does not carry out a variety of mechanical experiments for analysis. In this paper, the basic mechanical experiments will be used to explore what kind of weakening law of the mechanical properties of rocks under the influence of liquid nitrogen will be.

2. Experiment on Mechanical Properties of Granite

2.1. Test Equipment and Test Methods. The test contents include a uniaxial compression test, the Brazilian split test, and a three-point bending test. The granite specimen used in the uniaxial compression test is a standard cylindrical specimen with a height of 100 mm and a diameter of 50 mm. Granite samples were mined from Xuzhou, China. The instrument used in the test is domestic TAWD-2000. This is an electrohydraulic servo testing system for rock mechanical properties. This system has many kinds of functions. It can be used for uniaxial, triaxial, direct shear, and creep tests of rocks. It can also calculate various rock mechanical parameters. According to the joint operation of the systems, uniaxial compression tests can be conducted. For the Brazil splitting test, a Brazilian disk specimen with 25 mm thickness and 50 mm diameter is employed. Use this sample to prepare for the split test. The test is also carried out by using TAWD-2000. A semidisk sample with a thickness of 30 mm, diameter of 76 mm, manual slit length of 14 mm, and slit center perpendicular to the bottom diameter is used in the three-point bending test. The test equipment used in three-point bending test is the CSS-88020 universal testing machine. The main purpose of using this experimental equipment is to ensure the accuracy of the experiment. Because of the mechanical properties of granite itself, the experimental effect of using the CSS-88020 universal testing machine is more accurate than that of the domestic TAWD-2000 testing system. The CSS-88020 universal testing machine can provide a peak pressure of 20 KN. Because its control accuracy is very high, no prestress is applied in advance during the experiment. The experimental equipment can independently clear the mechanical data when contacting, which is convenient for the progress of the experiment. Therefore, accurate load displacement curves can be obtained. When controlling the displacement, it can be accurate to 0.001 mm. The CSS-88020 universal testing machine can automatically test after the parameters are set, until the rock sample is damaged.

2.2. Test Method. The granite samples used in the experiment are all pretreated. In order to reduce the heterogeneity of granite, all samples are from the same rock. After processing, all granite samples are stored with plastic wrap for later use. The experiment was divided into six groups: untreated at room temperature (25°C), room temperature+liquid nitrogen cooling, heated to 100°C+liquid nitrogen cooling, heated to 200°C+liquid nitrogen cooling, heated to 300°C +liquid nitrogen cooling, and heated to 400°C+liquid nitrogen cooling. All experimental groups included two kinds of samples, which were represented by 25-1 non, 25-2 non, 25-1, 25-2, 100-1, 100-2, 200-1, 200-2, 300-1, 300-2, 400-1, and 400-2.

(1) Treatment of samples: the initial group (25-1 non, 25-2 non) as the control group did not do any treatment. "25-1 untreated" and "25-1 non" refer to the same rock sample. Other groups were treated with high-temperature heating and liquid nitrogen cooling. High-temperature heating refers to continuous heating for three hours after the sample is heated to the predetermined temperature, and liquid nitrogen cooling refers to soaking for one hour each time. In order to avoid damage to rock caused by excessive heating rate, the heating rate remains unchanged, and the heating rate is 5°C/min.

(2) The process of experimental loading: force control method is adopted, which is the loading method of uniaxial experiment. It should be noted that the control speed should reach 100 N/s until the experiment is completed. The method of displacement control is adopted, which is the loading mode of Brazil splitting experiment. It should be noted that the control speed should reach 0.005 mm/s until the experiment is completed. The displacement control method is also the loading method of three-point bending test. It should be noted that the control speed should reach 0.005 mm/s until the experiment is completed. Broken rock samples of these rocks need to be preserved for subsequent analysis after all experiments are completed.

2.3. Mechanical Property Test Results

2.3.1. Uniaxial Compression Test Results. Many experimental information can be obtained from the test results, and the law of rock fracture can also be seen. It reflects the change of rock from initial loading to final fracture, as well as their correlation. In this experiment, we can understand the different stresses and strains of granite under liquid nitrogen and draw relevant conclusions. Generally speaking, in the uniaxial compression experiment of granite, the stress-strain curve will go through four different stages.

(1) The first stage is the initial compaction stage of granite: as a natural rock, granite is formed by magma condensation. Therefore, there must be a few initial cracks and pores between its internal particles. At the initial stage of loading on granite, the cracks between these initial cracks and pores will be gradually compacted with the increase of external load, and the gaps will be gradually closed. In the initial compaction stage of granite, the stress-strain curve is convex downward. The growth of stress is relatively slow, and the deformation is large as strain rises. The increase of rock stress is nonlinear. The longer the initial compaction stage of granite is, the more original fractures and pores are in granite

(2) The second stage is the elastic stage of granite: in this stage, the original fractures and pores have been completely closed. At this stage, the stress-strain curve of rock exhibits linear progression. According to some of the samples, we can get that the stress continues to increase linearly after the stress of some samples decreases in the elastic stage. Although the rock will be irreversibly damaged, the linearity of the curve remains unchanged at this time, which is still a linear state. The duration of the elastic stage of granite reflects the characteristics of rock strength. Generally speaking, the longer the duration, the higher the rock strength. On the contrary, the shorter the duration of the elastic stage of granite, the lower the rock strength

(3) The third stage is the crack propagation stage of granite: with the increasing external load, the internal damage and fracture of granite become more and more, and new cracks begin to develop. These cracks continue to extend and develop, eventually

leading to the rock fracture. Some granites are composed of granular particles, so there is a certain brittleness. The third stage is only shown before the peak stress, which accounts for a small proportion in the whole stress-strain curve of granite and is not easy to distinguish. It is close to the peak stress, which is shown in the section before the peak stress

(4) The fourth stage is the failure stage of granite: the granite has been damaged. When the external load reaches the peak strength of granite, the granite sample will undergo instant spalling or splitting failure, and the stress will drop sharply from the peak point to zero. At this time, the granite sample has been damaged

Figure 1 shows that the stress-strain curves of twelve rock samples are, respectively, given for six experimental groups: untreated at room temperature (25°C), room temperature+liquid nitrogen cooling, heated to 100°C+liquid nitrogen cooling, heated to 200°C+liquid nitrogen cooling, heated to 300°C+liquid nitrogen cooling, and heated to 400°C+liquid nitrogen cooling.

In the initial compaction stage of granite, when the temperature is the same, the compression stage of granite samples treated with liquid nitrogen is significantly increased than that of granite samples not treated with liquid nitrogen. This is because more cracks appear in the granite under the effect of liquid nitrogen, so it takes longer to compact these crack pores, and the initial compaction stage becomes longer. In addition, the mechanical properties of rocks with initial temperatures of 300°C and 400°C are obviously weakened under the treatment of liquid nitrogen, such as the peak stress is greatly reduced, which indicates that the weakening effect of liquid nitrogen on rocks with higher temperatures is more obvious. When low-temperature liquid nitrogen contacts high-temperature granite, the huge temperature difference between the two will cause stress between rock mineral particles, thus causing damage to the interior of the rock. The connection between axial stress and circumferential strain is seen in Figure 2.

2.3.2. Brazil Splitting Test Results. An important mechanical property index can be obtained from Brazilian splitting which is tensile strength. The tensile strength refers to the maximum bearing capacity under static tension. Generally speaking, under the action of external load, the tensile stress at a certain position in the rock in a certain direction exceeds the maximum bearing capacity, that is, the tensile strength, and the rock specimen will be damaged. This failure will lead to new cracks or new pores on the surface or inside of the rock. In view of this, the influence of rock tensile strength plays an important role in production. It will have a direct impact on the process of rock fracturing under pressure in engineering practice; that is, it will lead to the generation and development of cracks. In order to develop the engineering technology of liquid nitrogen assisted mining of dry hot rock, it is necessary to master the change rule of rock tensile strength under liquid nitrogen treatment. Figure 3 shows the load displacement curve of rock under different treatment methods in Brazil splitting experiment.

According to Figure 3, the axial load axial displacement curves of granite samples in different states are different. The curve of granite without liquid nitrogen treatment is relatively smooth, while that of granite with liquid nitrogen treatment is relatively steep, which indicates that new cracks and fissures are generated in the interior of granite with liquid nitrogen treatment, which indicates that liquid nitrogen has weakened the mechanical properties of granite.

2.3.3. Three-Point Bending Test Results. Fracture toughness is an important physical and mechanical parameter of rock and a particularly important mechanical index in rock fracture mechanics. An effective way to obtain fracture toughness is through the three-point bending test, which is widely used. The size of fracture toughness reflects the resistance of rock to cracks in the process of crack generation and crack propagation. It is an index that requires great attention in the process of rock fracturing. When using liquid nitrogen fracturing technology to exploit dry hot rock, the change rule of fracture toughness can also provide guidance for it. Figure 4 shows the load displacement curve of rock under different treatment modes in three-point bending test.

Figure 4 shows that the curve of granite treated with liquid nitrogen is different from that of granite untreated. This is because after liquid nitrogen treatment, the cracks and voids inside the granite increase, which affects the mechanical properties of the rock and leads to this difference. At the same time, when the temperature reaches 300°C and 400°C, the effect of liquid nitrogen is more obvious, demonstrating that the impact of liquid nitrogen is more noticeable at higher temperatures.

2.4. Summary of Mechanical Parameters of Granite Samples in Different States

2.4.1. Compressive Strength. The compressive strength of granite can be obtained from the data of uniaxial compression test. According to the knowledge of material mechanics, the compressive strength of granite is the magnitude of the peak stress in the uniaxial compression experiment. The compressive strength of each sample is obtained according to the test data, and the average compressive strength of six groups of test groups is calculated. Table 1 shows the compressive strength data of different samples, and the statistical graph of the compressive strength of rock samples after various treatments is shown in Figure 5.

2.4.2. Tensile Strength. Amadei et al. [35] studied the calculation method of tensile strength, which can be calculated by the following formula:

$$\sigma_t = \frac{2P_{max}}{\pi DB}. \quad (1)$$

In this formula, σ_t represents the tensile strength, that is, the required tensile strength of Brazil splitting. P_{max} is the peak load of the specimen. D is the diameter of the disc; B is the thickness of the disc.

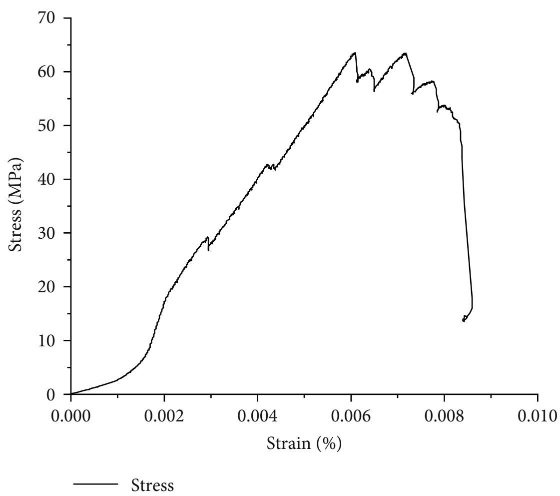

(a) 25-1 untreated

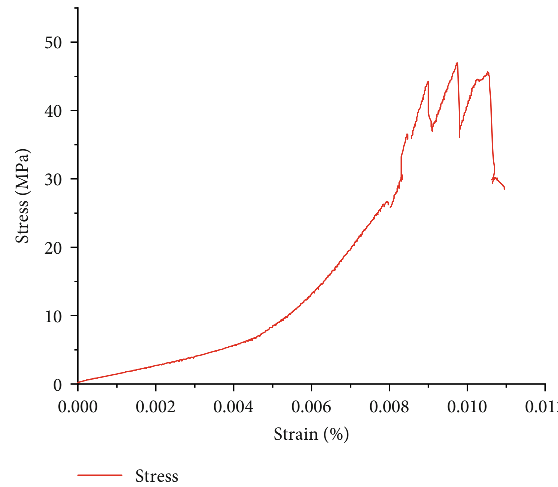

(b) 25-2 untreated

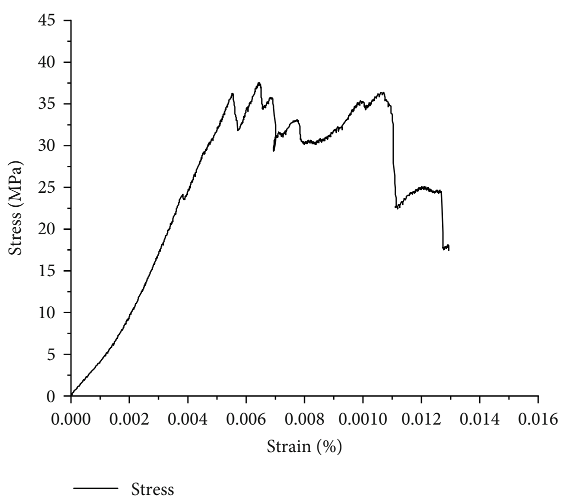

(c) 25-1

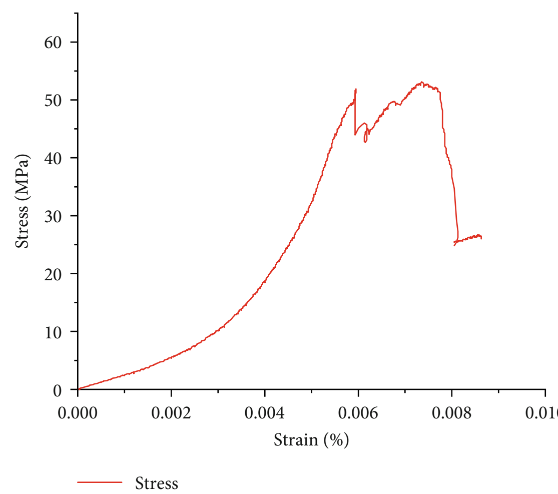

(d) 25-2

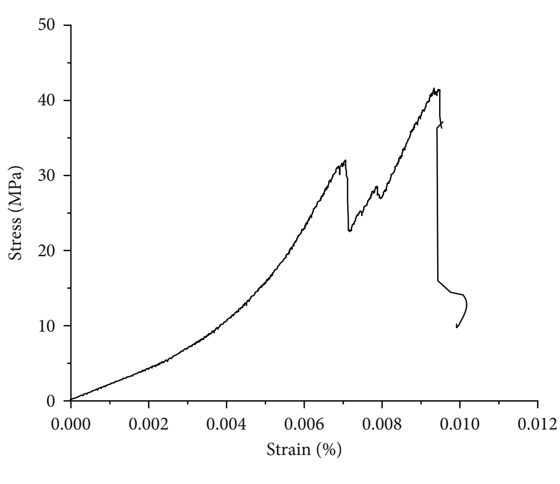

(e) 100-1

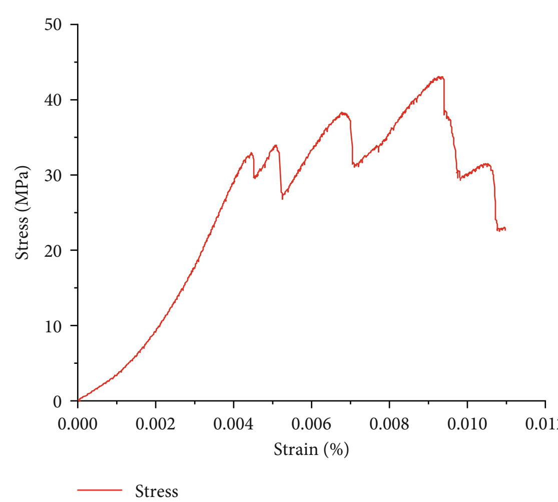

(f) 100-2

Figure 1: Continued.

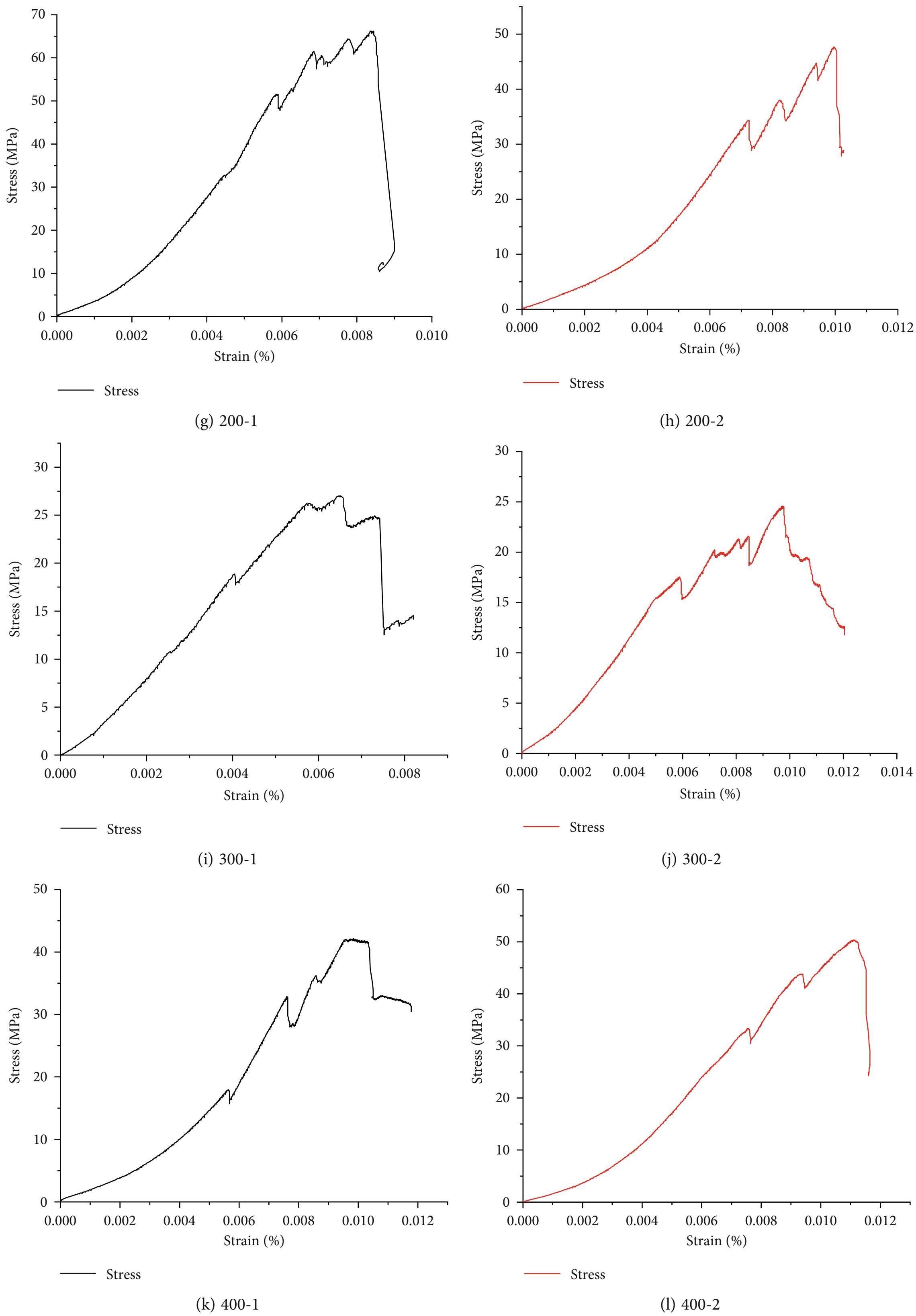

Figure 1: The stress-strain curves of twelve rock samples.

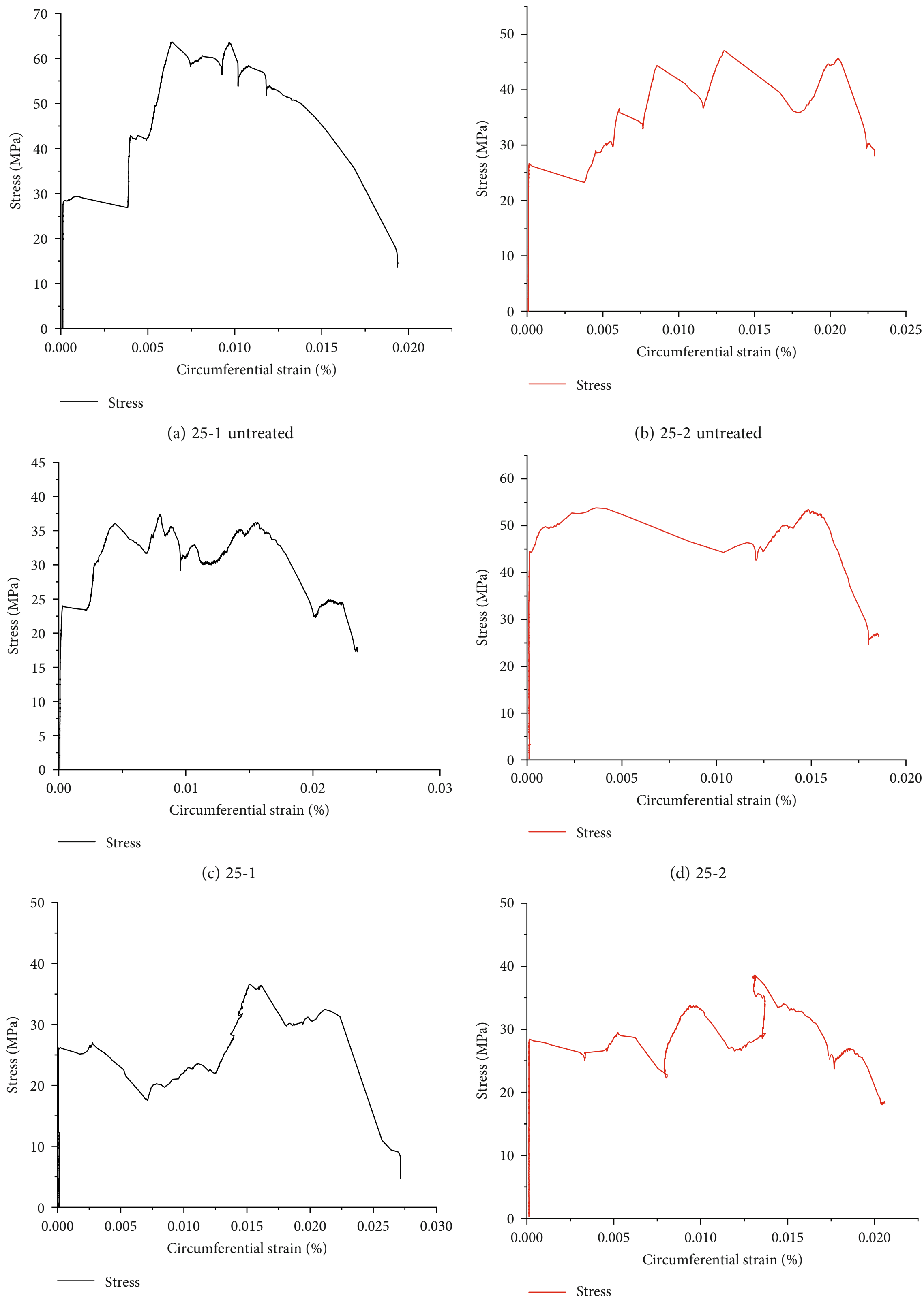

(a) 25-1 untreated

(b) 25-2 untreated

(c) 25-1

(d) 25-2

(e) 100-1

(f) 100-2

Figure 2: Continued.

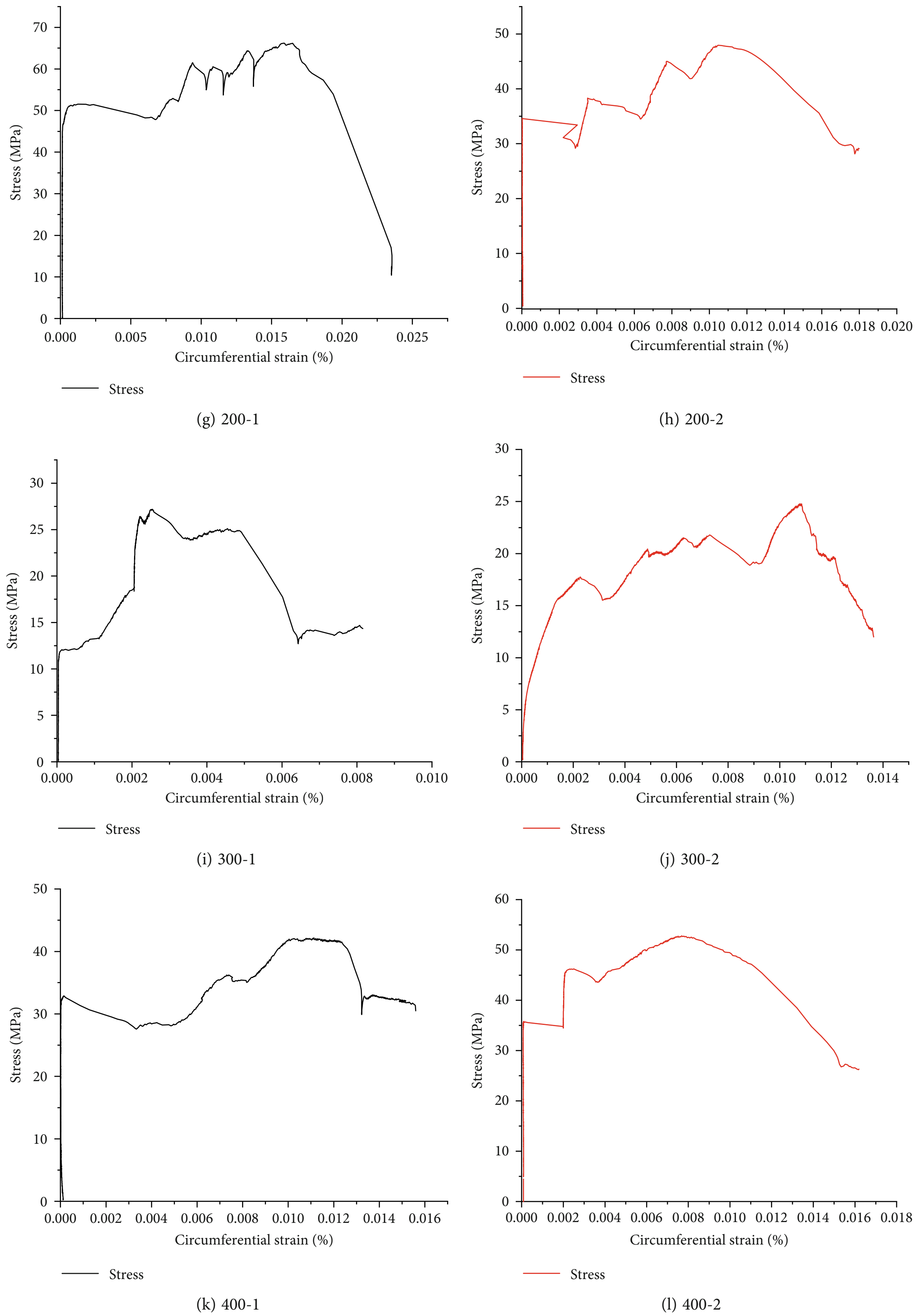

FIGURE 2: The connection between axial stress and circumferential strain of rock sample.

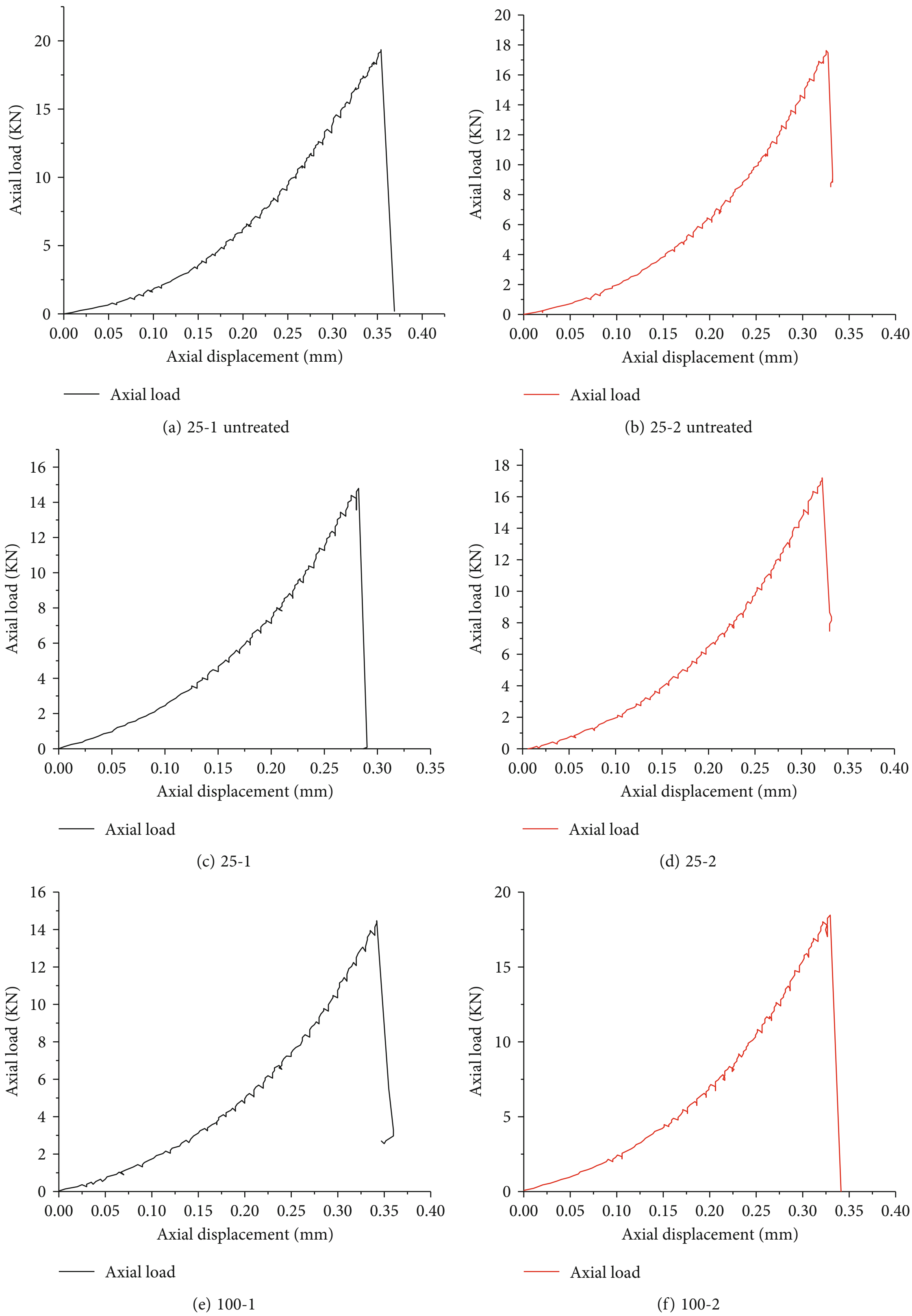

Figure 3: Continued.

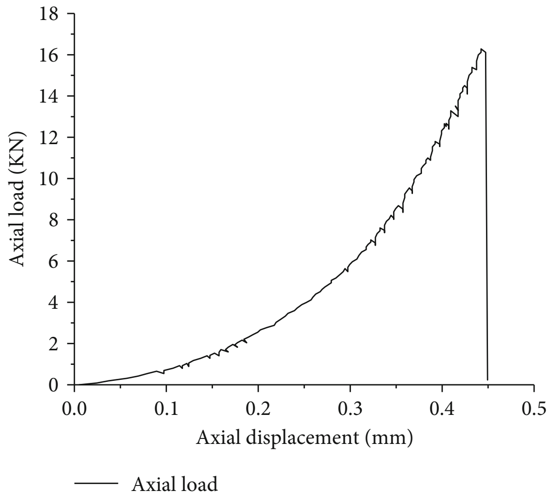

(g) 200-1

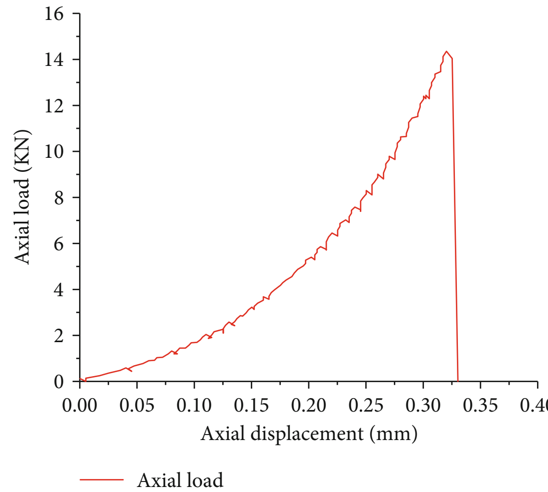

(h) 200-2

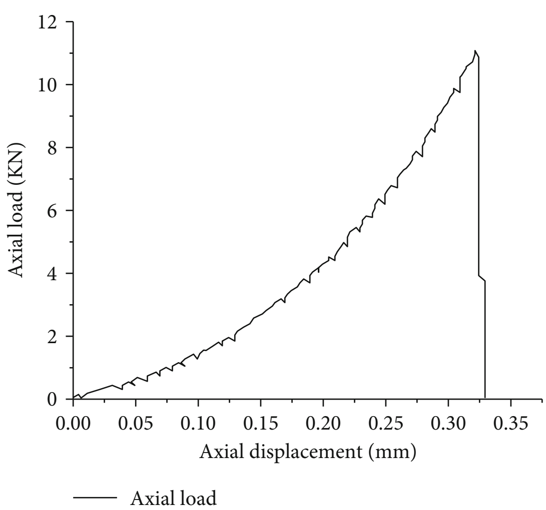

(i) 300-1

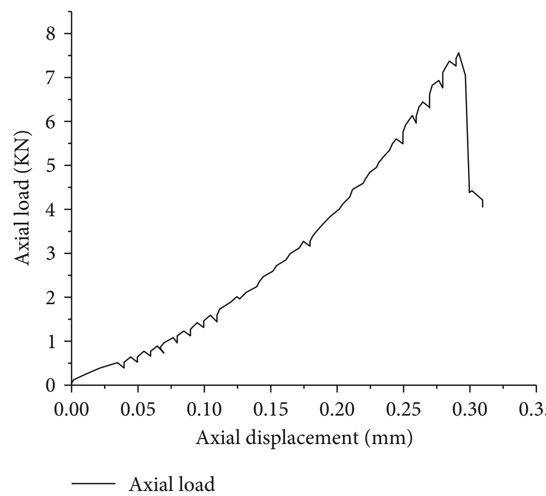

(j) 400-1

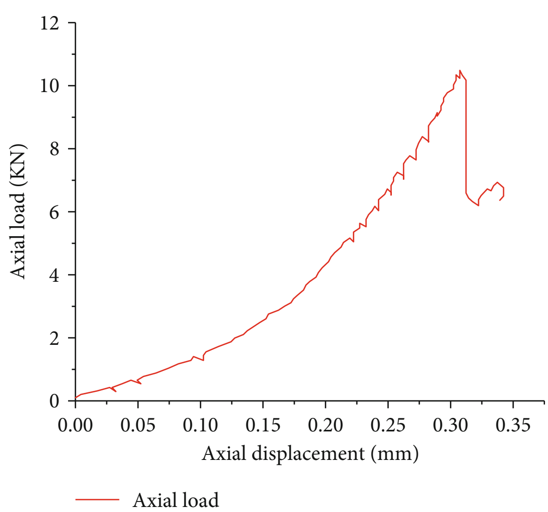

(k) 400-2

Figure 3: The load displacement curve of rock under different treatment methods in Brazil splitting experiment.

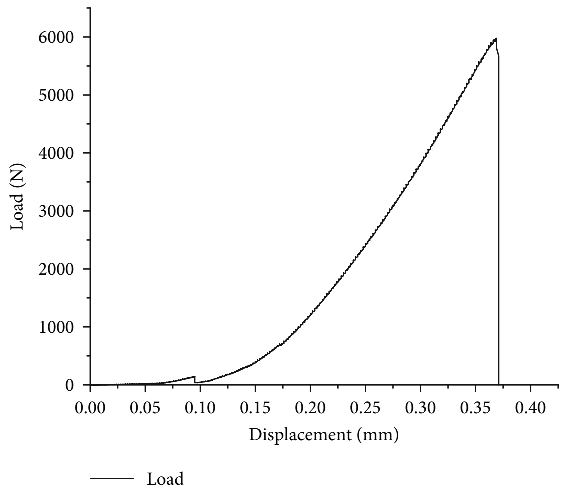

(a) 25-1 untreated

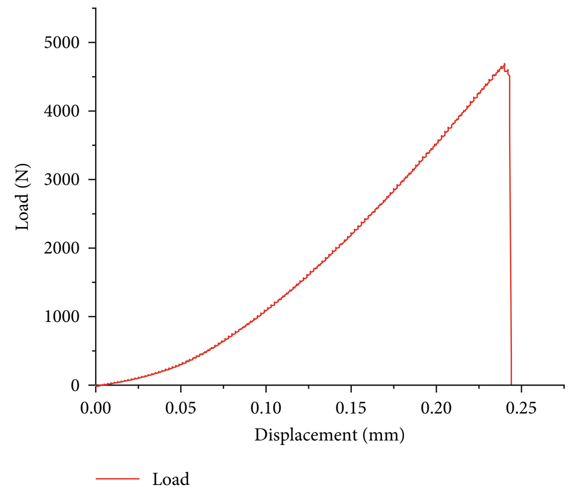

(b) 25-2 untreated

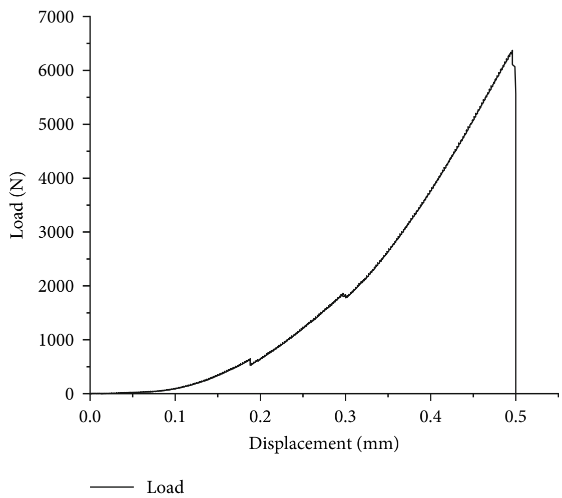

(c) 25-1

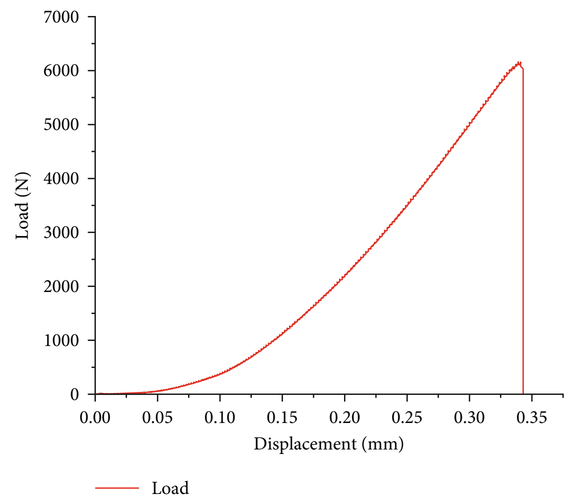

(d) 25-2

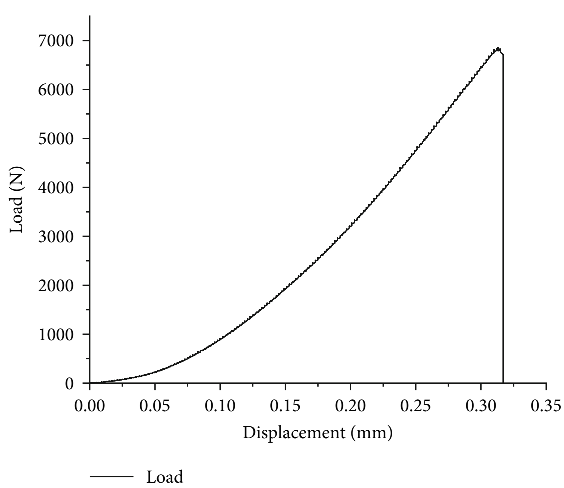

(e) 100-1

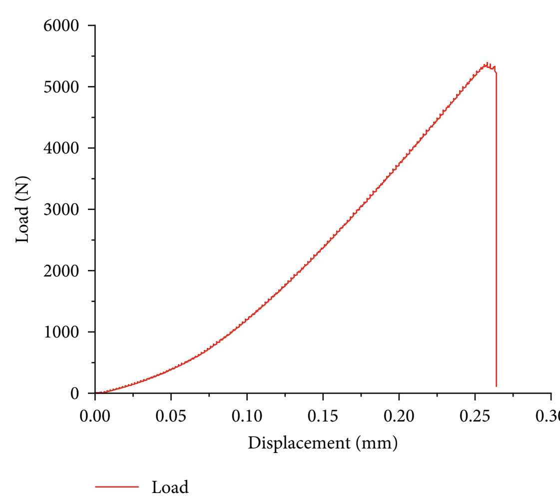

(f) 100-2

FIGURE 4: Continued.

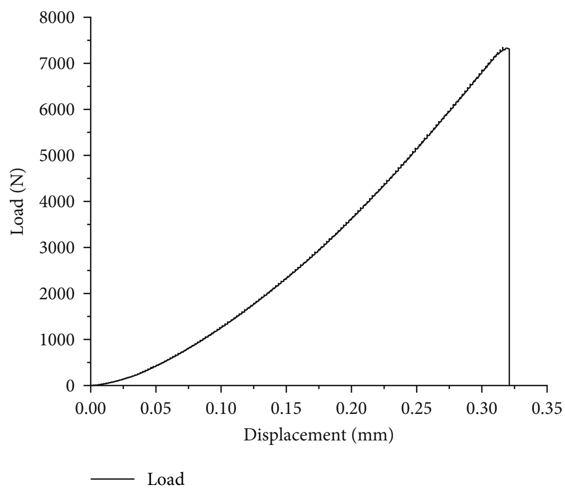

(g) 200-1

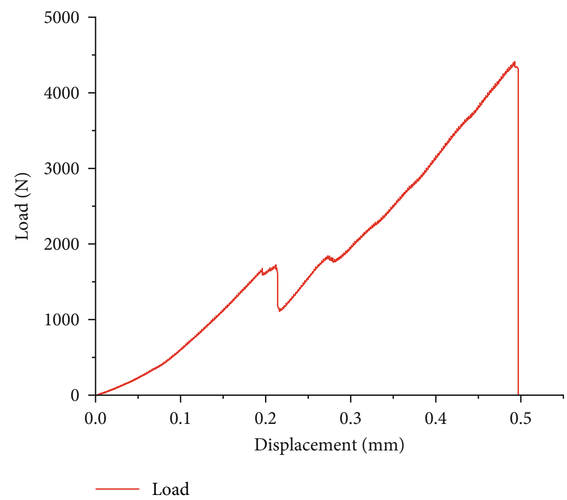

(h) 200-2

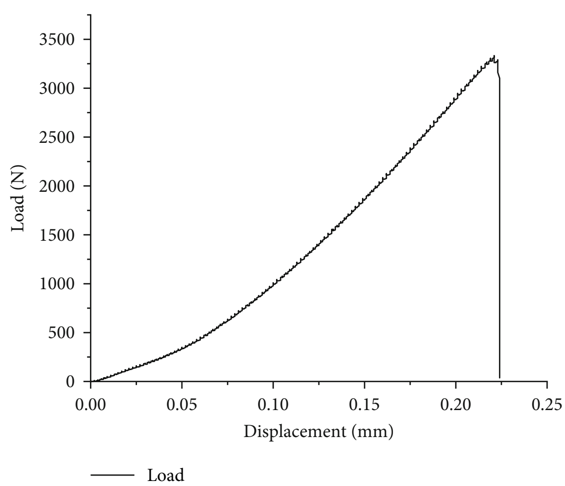

(i) 300-1

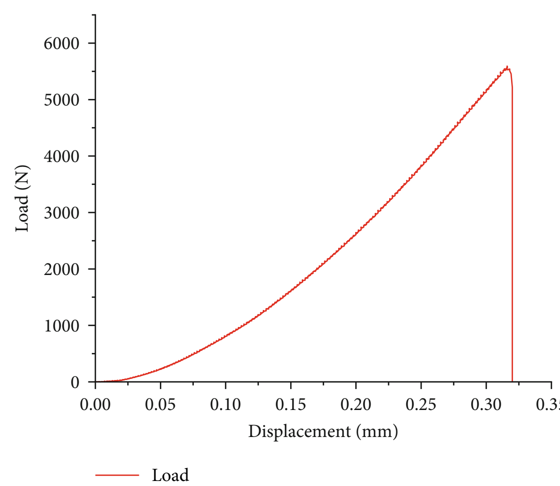

(j) 300-2

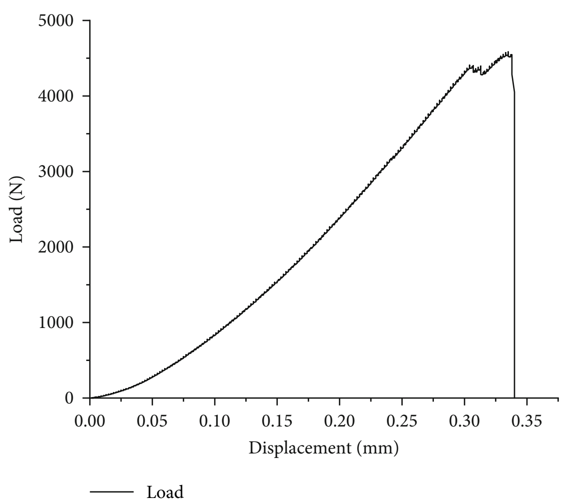

(k) 400-1

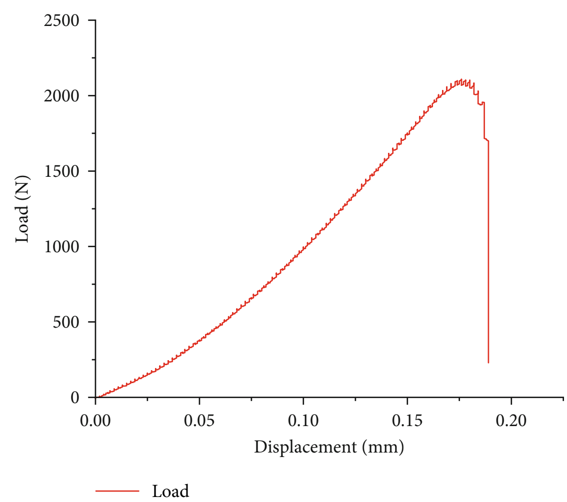

(l) 400-2

Figure 4: Load displacement curve of rock under different treatments in three-point bending test.

According to this formula, the tensile strength of each sample is calculated, and the average tensile strength of six groups of test data is calculated. Table 2 shows the tensile strength data of different samples, and the statistical chart of the tensile strength of rock samples after various treatments is shown in Figure 6.

Table 1: Compressive strength data of different specimens.

Rock sample name	Compressive strength (MPa)	Average value (MPa)
25-1 non	64.65	56.195
25-2 non	47.74	
25-1	39.86	47.86
25-2	55.86	
100-1	44.09	44.83
100-2	45.57	
200-1	68.46	59.23
200-2	50.00	
300-1	29.66	28.36
300-2	27.05	
400-1	44.36	48.58
400-2	52.80	

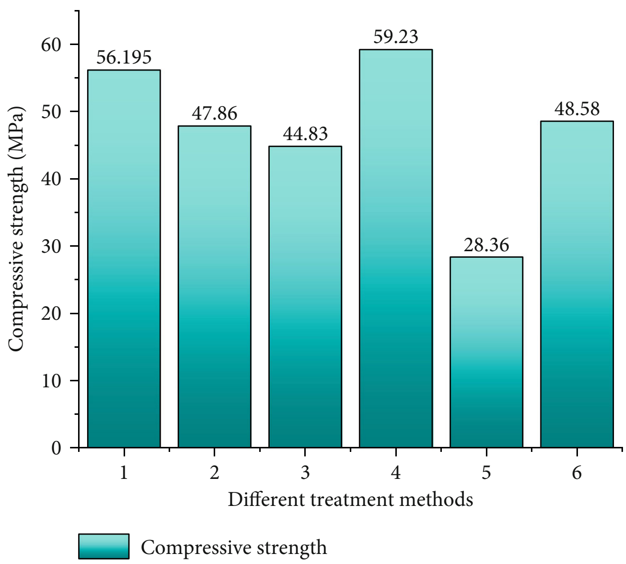

Figure 5: The statistical graph of the compressive strength of rock samples after various treatments.

Table 2: Tensile strength data of different specimens.

Rock sample name	Tensile strength (MPa)	Average value (MPa)
25-1 non	9.77	9.4
25-2 non	9.03	
25-1	7.69	8.275
25-2	8.86	
100-1	7.30	8.335
100-2	9.37	
200-1	8.16	7.735
200-2	7.31	
300-1	5.56	5.56
300-2	5.56	
400-1	3.87	4.535
400-2	5.20	

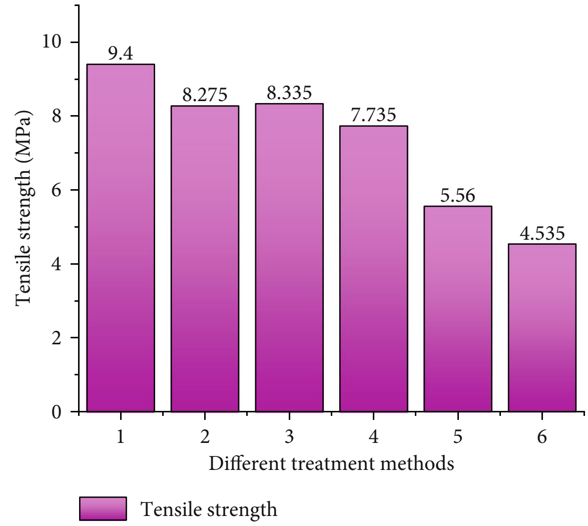

Figure 6: The statistical chart of the tensile strength of rock samples after various treatments.

2.4.3. Elastic Modulus. The elastic modulus reflects the degree of difficulty of granite deformation, which has great reference value for the deformation analysis of rock. Table 3 shows the elastic modulus of different samples, and the elastic modulus of rock samples treated using various techniques is shown in Figure 7.

2.4.4. Poisson's Ratio. Poisson's ratio is also an important mechanical parameter of granite. It is also called transverse strain coefficient, which reflects the transverse deformation of granite material and the degree of mutual influence of granite deformation in different directions. In the above, we have drawn the stress-strain curves and stress-strain curves of uniaxial compression experiments. Poisson's ratio of each test sample is obtained through analysis and calculation, and average Poisson's ratio of six groups of test data is obtained. Table 4 shows the Poisson's ratio of different samples, and Figure 8 shows Poisson's ratio of rock samples with different treatment methods.

2.4.5. Fracture Toughness. It can be seen from the above that fracture toughness is an important physical and mechanical parameter of rock and a particularly important mechanical index in rock fracture mechanics. An effective way to obtain fracture toughness is through three-point bending test, which is widely used. The size of fracture toughness reflects the resistance of rock to cracks in the process of crack generation and crack propagation. It is an index that requires great attention in the process of rock fracturing. According to the relevant knowledge of fracture mechanics, we can know that the value of rock fracture toughness is the value of stress intensity factor at the crack tip when granite cracks. It can be seen from literature that Lim et al. [36] proposed a formula for calculating this stress intensity factor:

$$K_1 = \frac{P}{DB}\sqrt{\pi\tau}Y_1\left(\frac{\tau}{R}, \frac{S}{R}, \alpha\right). \tag{2}$$

Table 3: The elastic modulus of different samples.

Rock sample name	Elastic modulus (GPa)	Average value (GPa)
25-1 non	11.84	9.565
25-2 non	7.29	
25-1	6.53	7.635
25-2	8.74	
100-1	6.73	8.115
100-2	9.50	
200-1	11.17	10.02
200-2	8.87	
300-1	5.22	4.415
300-2	3.61	
400-1	4.02	4.68
400-2	5.34	

Table 4: Poisson's ratio of different samples.

Rock sample name	Poisson's ratio	Average value
25-1 non	0.55	0.545
25-2 non	0.54	
25-1	0.42	0.450
25-2	0.48	
100-1	0.51	0.575
100-2	0.64	
200-1	0.40	0.470
200-2	0.54	
300-1	0.58	0.530
300-2	0.48	
400-1	0.50	0.475
400-2	0.45	

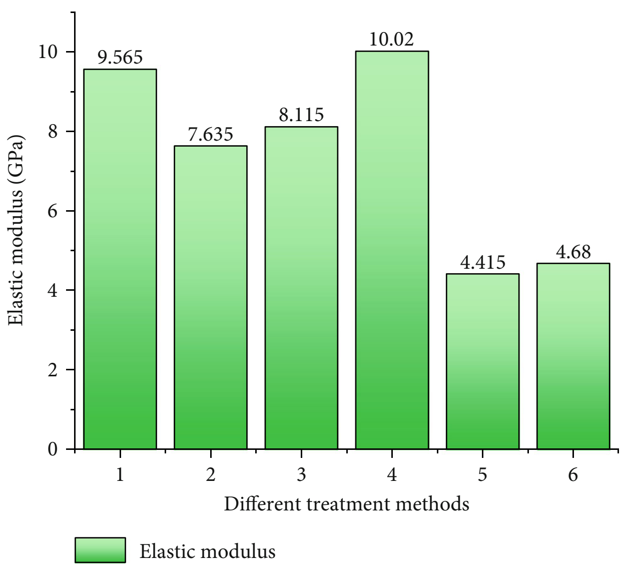

Figure 7: The elastic modulus of rock samples treated using various techniques.

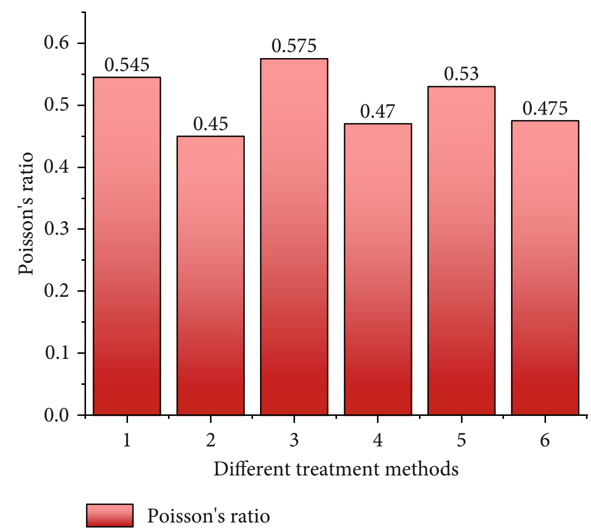

Figure 8: Poisson's ratio of rock samples with different treatment methods.

In the formula, K_1 represents the stress intensity factor without unit; P is the peak load; D is the diameter of the disc; B is the thickness of the disc; Y_1 and Y_{11} are dimensionless geometric factors, which are related to the geometric dimensions of three-point bending specimens [37]. For general tensile rock fracture, $Y_1 = 3.61$ and $Y_{11} = 0$. The fracture toughness of each sample is calculated through analysis and calculation, and the average fracture toughness of six groups of test data is calculated. Table 5 shows the fracture toughness of different samples, and Figure 9 shows the fracture toughness of rock samples with different treatment methods.

According to the above summary diagram of mechanical parameters of granite in different states, we can find that under the action of liquid nitrogen, cracks and fissures between grains in granite further develop, and liquid nitrogen plays a role in promoting. It can be concluded that liquid nitrogen has obvious weakening effect on granite. It is not difficult to find that when the temperature reaches 300°C or 400°C, the effect of liquid nitrogen is the most obvious. At 300°C, the compressive strength of granite is reduced by about 50%, and the compressive strength is 28.36 MPa. At 400°C, the compressive strength is 48.58 MPa. For the tensile strength, there is a law of decreasing. The higher the temperature of granite is, the more obvious the weakening effect of tensile strength is. The lowest is 4.535 MPa at 400°C. For the elastic modulus, when the granite temperature is 300°C and 400°C, it also drops to the lowest, which is about 50% lower than the untreated rock sample. Poisson's ratio has no significant change. For the fracture toughness obtained from the three-point bending test, when the initial temperature of granite is 300°C and 400°C, the fracture toughness of rock sample decreases to the lowest, which is 1.725 MPa·m$^{1/2}$ and 1.295 MPa·m$^{1/2}$, respectively.

Table 5: The fracture toughness of different samples.

Rock sample name	Fracture toughness ($MPa \cdot m^{1/2}$)	Average value ($MPa \cdot m^{1/2}$)
25-1 non	2.31	2.06
25-2 non	1.81	
25-1	2.46	2.42
25-2	2.38	
100-1	2.65	2.37
100-2	2.09	
200-1	2.84	2.58
200-2	2.31	
300-1	1.29	1.725
300-2	2.16	
400-1	1.77	1.295
400-2	0.82	

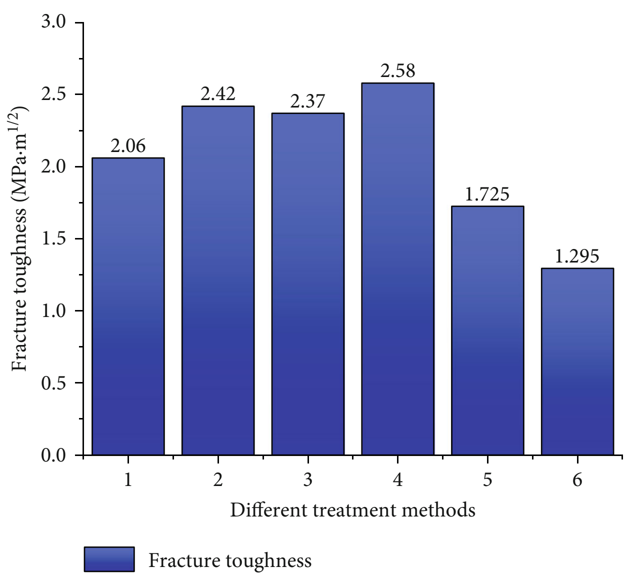

Figure 9: Fracture toughness of rock samples with different treatment methods.

3. Experimental Results of Acoustic Emission Characteristics of Granite

In order to obtain the acoustic emission information of high-temperature granite under the action of liquid nitrogen, the acoustic emission signals in the process of granite failure were collected. Figure 10 shows the variation of stress, ring count, and cumulative ring count of granite with time under different initial temperatures, and Figure 11 shows the variation of stress, energy count and cumulative energy count of granite with time under different initial temperatures.

From the analysis in Figures 10 and 11, we can draw these conclusions: in the uniaxial compression experiment, in the process of loading the granite, in the first stage, namely, the granite fissure compaction stage, the tiny fractures, and pores in the granite are gradually compressed until the volume becomes zero. In this interval, the signal of energy counting will be weakened. Since the number of energy signals at this stage is almost zero or single digit, the value of the cumulative energy count is basically unchanged, the growth rate is 0, and the slope of the growth rate is almost unchanged. In the second stage, the value of energy count will increase slightly. But the total value is still very low. At the end of this phase, the cumulative energy count began to increase slowly. This is because we are approaching the third stage. The third stage is the crack propagation stage of granite, and the energy count starts to rise rapidly. In the final stage of granite failure, the energy count jumped to the peak, and the cumulative energy count changed greatly. According to the comparison between the acoustic emission signal diagrams of granite at different initial temperatures, it can be seen that the mechanical properties of granite with higher initial temperature are weaker.

4. Energy Change of Granite

4.1. Change of Energy in Mechanical Test of Rock. The energy of rock is generally stored in the interior of rock, and its size is a process of gradual accumulation. However, when the energy inside the rock accumulates to a large extent, it will erupt from the inside of the rock, which is shown as rock collapse and flying from the macro level. This is called rock burst. Rock burst has a very bad impact on human rock engineering, and now, human technical means can not predict rock burst; rock burst has a great threat to human life and property safety. In addition to the accumulation of internal energy of the rock, external stress and other factors will also affect the energy of the rock. The energy of the rock will not change greatly if the stress around the rock does not change. However, if human construction or wind load, rain load, and other factors affect the surrounding rock pressure, it will change, which will cause the rock to receive a certain force; at this time, the energy inside the rock will change. According to the characteristic that the energy will change due to the change of external load, the energy change of granite in the mechanical property experiment can be explored through experiment conducted previously. The stress-strain curves of uniaxial compression tests were obtained from the mechanical properties of the three types of granites, axial load axial displacement curve of Brazilian splitting test, and load displacement curve of three-point bending test. These three curves can be used to analyze the energy change of granite in the mechanical property experiment.

According to the uniaxial compression experiment, the change of energy dissipation of granite with the increase of external stress can be analyzed [38]. According to formula (3), the calculation method of energy dissipation value in uniaxial compression test can be obtained.

$$U = \int \sigma_1 d\varepsilon_1, \tag{3}$$

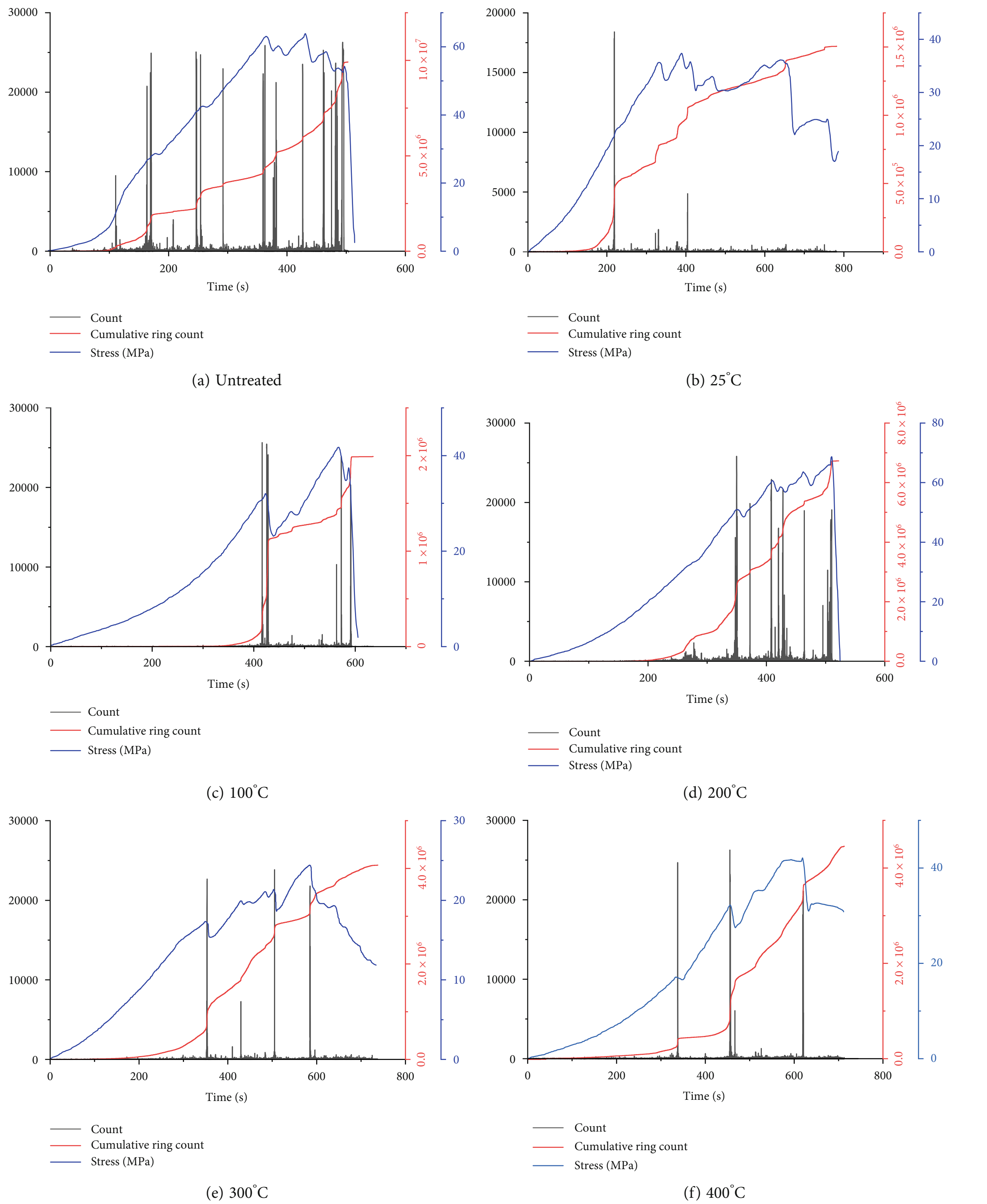

Figure 10: Variation of stress, ring count and cumulative ring count of granite with time under different initial temperatures.

where U represents energy, σ_1 represents differential of stress, and $d\varepsilon_1$ represents differential of strain.

Figure 12 shows that the energy of two groups of samples in uniaxial compression test changes as the stress increases.

According to the stress energy curve, with the increase of stress, the energy dissipation value is also increasing, and the two are positively correlated. The energy dissipation value of granite with liquid nitrogen treatment is obviously

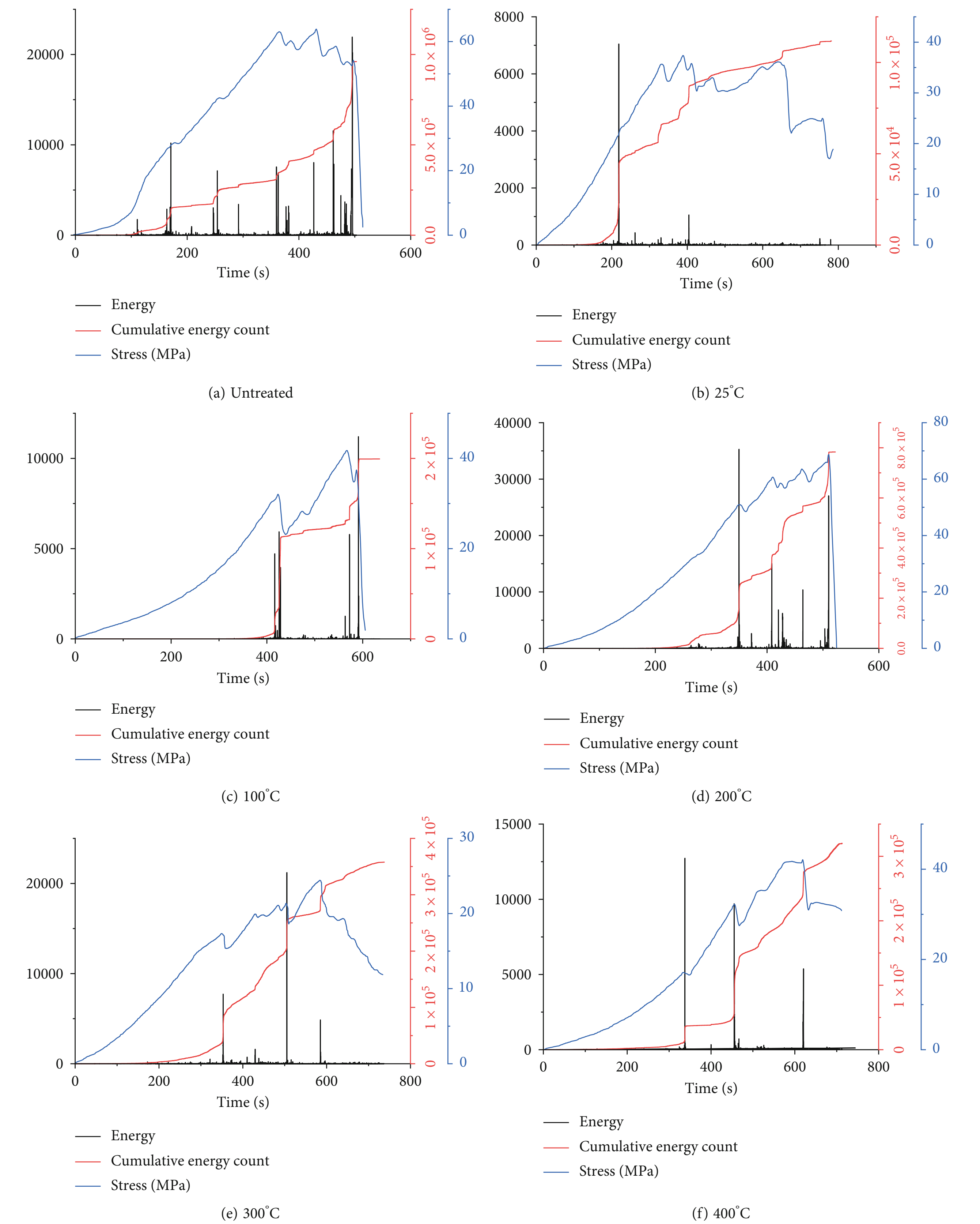

Figure 11: The variation of stress, energy count, and cumulative energy count of granite with time under different initial temperatures.

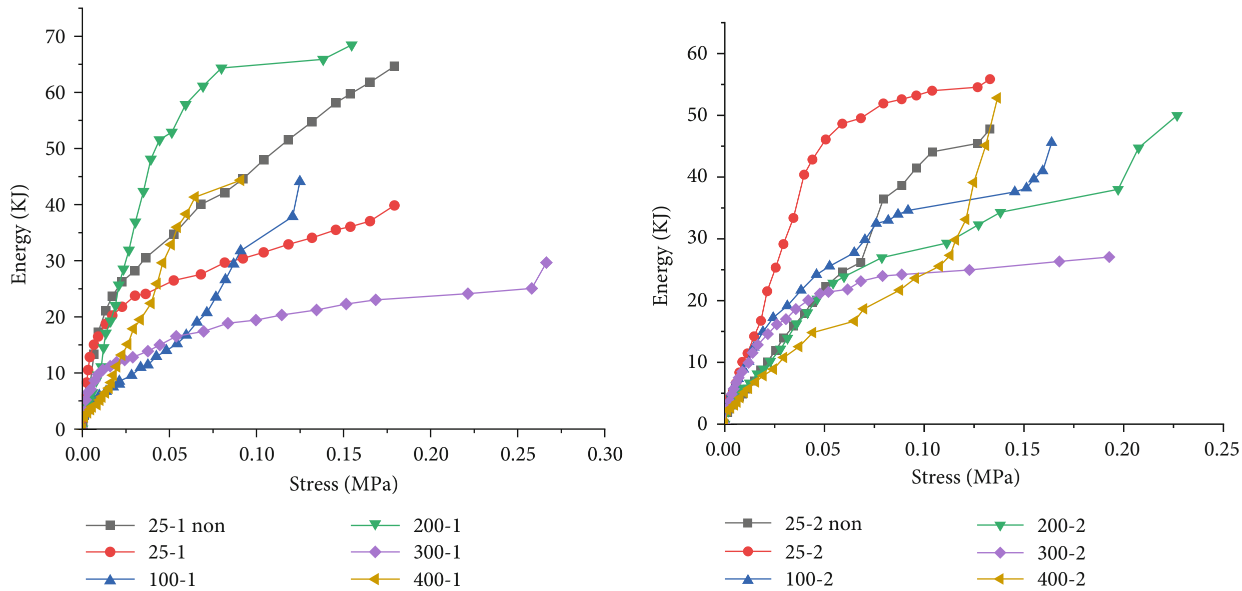

(a) Stress energy curve of uniaxial sample 1

(b) Stress energy curve of uniaxial sample 2

Figure 12: Stress energy curve of uniaxial compression test.

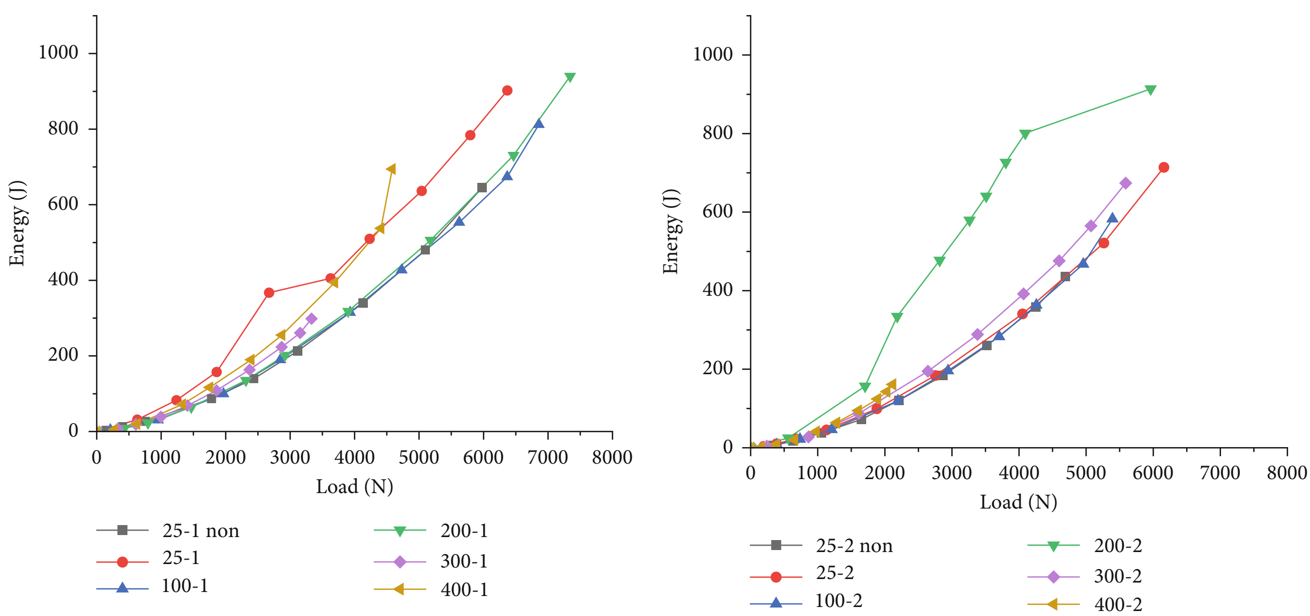

(a) Load energy curve of three-point bending sample 1

(b) Load energy curve of three-point bending sample 2

Figure 13: Load energy curve of three-point bending test.

greater than that of granite without liquid nitrogen treatment. From the perspective of temperature, under the same stress conditions, the higher the temperature of granite, the faster the energy dissipation value. This is because the higher the temperature is, the more obvious the weakening effect granite is.

The energy absorbed by rock can be analyzed with the change of external load on rock [39]. In case of rock failure, not only the dissipation of energy just analyzed will occur, but also the absorption and accumulation of energy.

According to formula (4), the energy absorbed by the rock can be calculated. The calculation method is the same as that of uniaxial compression test.

$$U = \int_0^{l_i} p_i dl, \tag{4}$$

where U represents energy, l_i represents displacement changing with time, p_i represents differential of load, and d l represents differential of displacement.

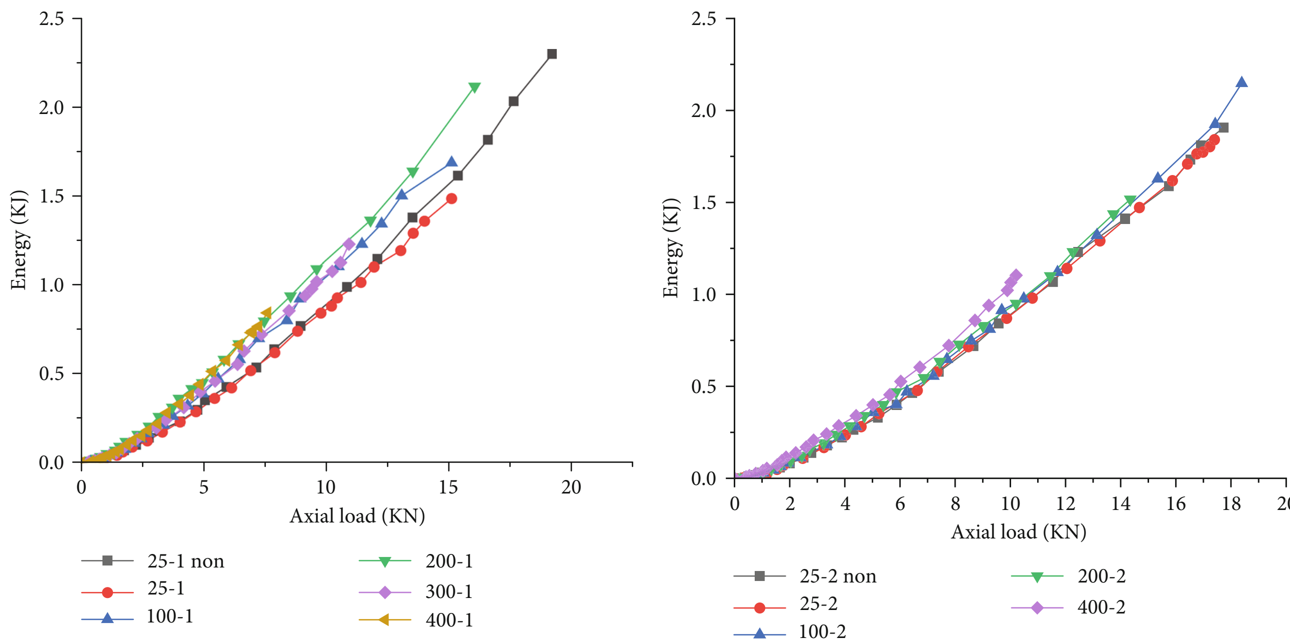

(a) Load energy curve of Brazil split sample 1 (b) Load energy curve of Brazil split sample 2

Figure 14: Axial load energy curve of Brazil splitting test.

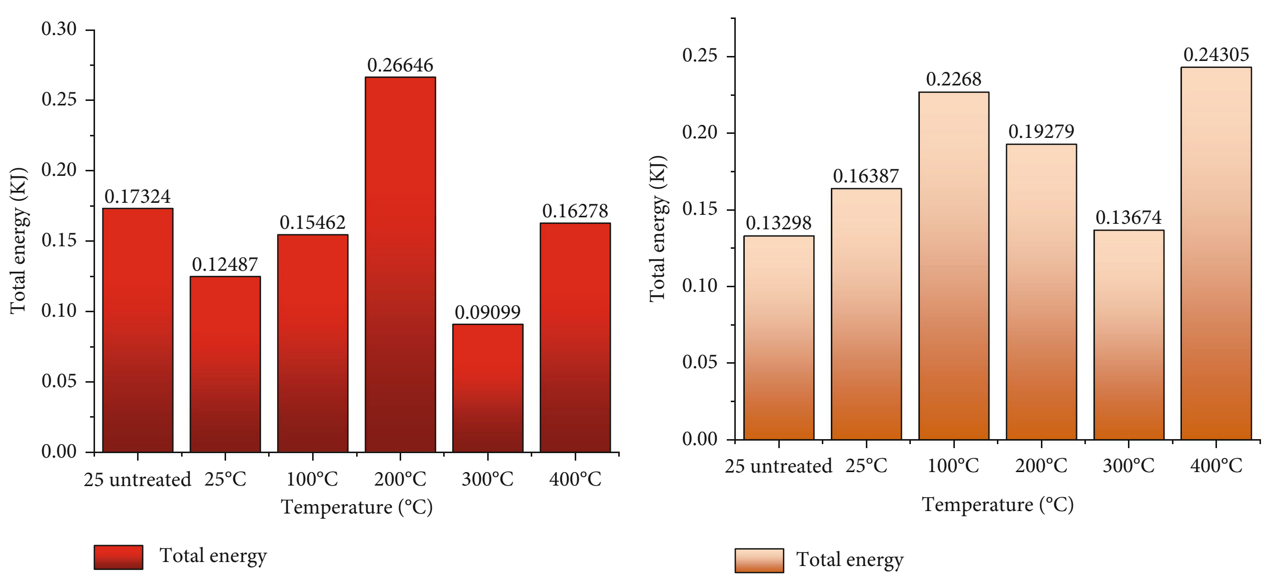

(a) Temperature and total energy statistic diagram of uniaxial compression sample 1 (b) Temperature and total energy statistic diagram of uniaxial compression sample 2

Figure 15: Temperature and total energy statistics of uniaxial compression test.

The change of energy with load in three-point bending test is shown in Figure 13.

The energy of Brazil splitting test varies with the axial load as shown in Figure 14. Figure 13 shows the change of energy with load in the three-point bending test. It can be seen from Figures 13 and 14 that the energy absorbed by granite increases with the increase of stress.

4.2. Relationship between the Total Energy Absorbed or Released by Granite at the Peak Stress and Its Temperature. Combining the total energy absorbed or released by granite at the peak stress with temperature, the situation in uniaxial compression test is shown in Figure 15.

The situation in Brazil splitting test is shown in Figure 16.

In the three-point bending test, the situation is shown in Figure 17.

Under high-temperature conditions, such as 300°C and 400°C, the total energy released or absorbed by granite treated with liquid nitrogen is the smallest. Therefore, we

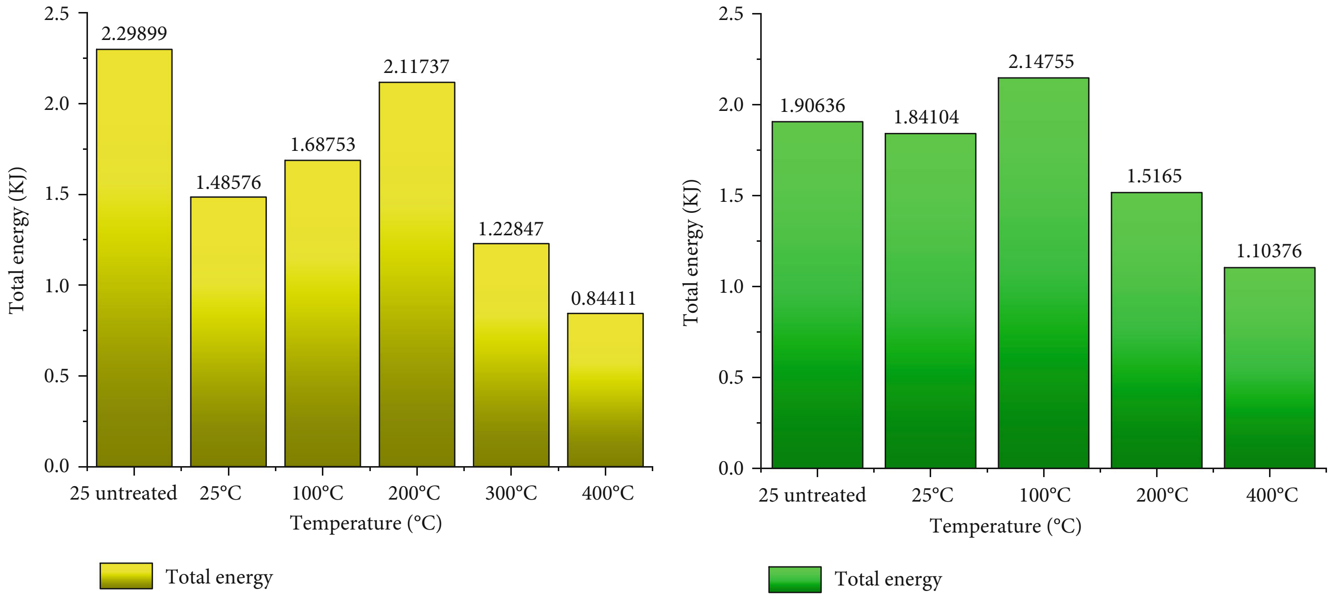

(a) Statistical diagram of temperature and total energy of Brazil splitting sample 1

(b) Statistical diagram of temperature and total energy of Brazil splitting sample 2

Figure 16: Statistical diagram of temperature and total energy of Brazil splitting experiment.

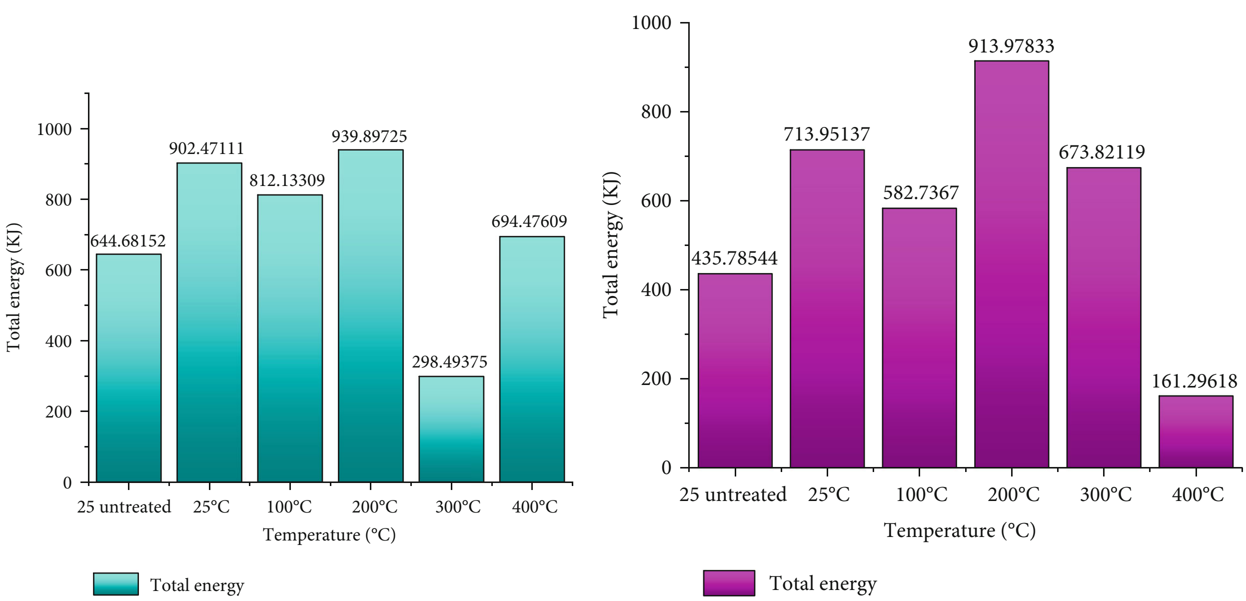

(a) Temperature and total energy statistics of three-point bending sample 1

(b) Temperature and total energy statistics of three-point bending sample 2

Figure 17: Temperature and total energy statistics of three-point bending test.

can draw a conclusion similar to the previous conclusion: liquid nitrogen has an obvious weakening effect of granite, and the higher the temperature is, that is, when it reaches 300˚C or 400˚C, the weakening effect is most obvious.

4.3. Relationship between Total Energy Released or Absorbed by Granite and Peak Stress or Load. Scatter plots of the peak stress or energy released or absorbed at the load under the three kinds of experiments are drawn with origin software and fitted. The results are shown in Figure 18.

The energy changes of the three experiments are positively correlated with the peak stress or load. The larger the peak stress or load, the more total energy absorbed or dissipated. Therefore, the use of liquid nitrogen for treatment can reduce the energy loss during the development of dry hot rocks. Liquid nitrogen has an obvious role in

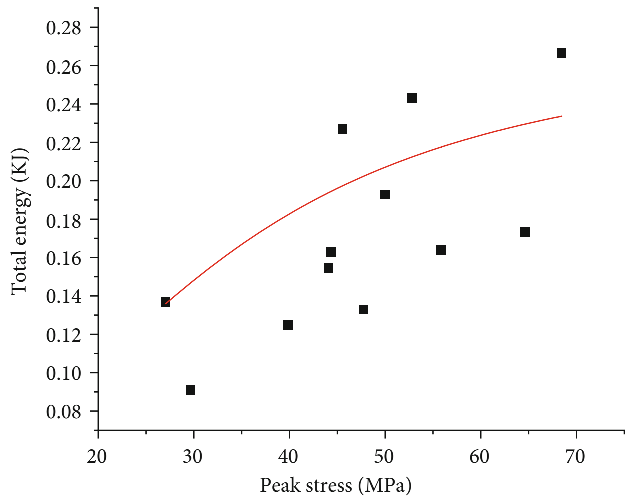

(a) Relationship between peak stress and total energy dissipation in uniaxial compression test and fitting curve

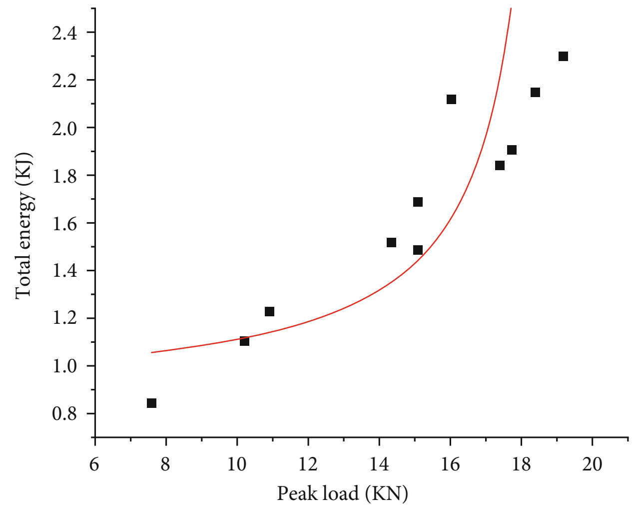

(b) Relationship between peak load and total energy absorption in Brazil splitting experiment and fitting curve

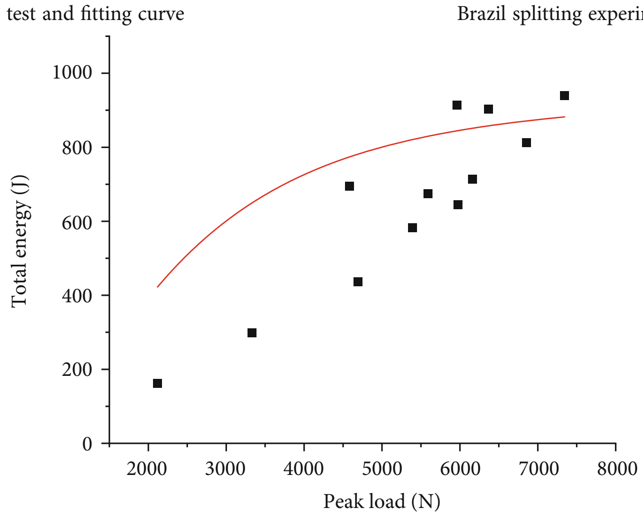

(c) Relationship between peak load and total energy absorption in three-point bending test and fitting curve

FIGURE 18: Fitting relationship between peak load and total absorbed energy in different tests.

reducing energy consumption. After the granite is cooled by liquid nitrogen, many tiny cracks will be generated inside the granite.

5. Conclusion

In this paper, the characteristics of rock mechanical properties weakening under the action of liquid nitrogen are investigated. Through three groups of experiments, the mechanical behavior of rock under the action of liquid nitrogen is analyzed, and various mechanical parameters of granite rock samples are calculated and summarized. According to the test results, we know that the mechanical properties of granite samples treated with liquid nitrogen are weaker than those without liquid nitrogen treatment. The higher the initial temperature, the greater the temperature difference between granite and liquid nitrogen. Liquid nitrogen not only has fracturing damage on granite samples but also has thermal stress on granite samples. If the temperature difference between the two is larger, the heat energy released during the combination will be higher. The higher the heat energy is, the greater the damage to granite will be. So liquid nitrogen can also be used for fracturing dry hot rocks, and the temperature of dry hot rocks is relatively high, so liquid nitrogen will have a very obvious damage effect. It is feasible to use liquid nitrogen as fracturing fluid for dry hot rock fracturing. The research results can provide some scientific guidance for the development and utilization of geothermal energy.

Data Availability

The data used to support the findings of this study are included within the article.

Conflicts of Interest

The authors declare that they have no conflicts of interest.

Acknowledgments

Dr. Xin Liang has contributed to the analysis of experimental data and the exploration of the relationship between energy and stress in the manuscript. We are greatly appreciative of his significant contributions to this research. The authors are grateful to the financial support from the National Natural Science Foundation of China (52274096, 12202353, and 12002270), the Key Research and Development Program of Shaanxi Province, China (2022ZDLSF07-06 and 2023-YBSF-369), the China Postdoctoral Science Foundation (2020M683686XB, 2020M673451, 2021T140553, and 2021M692600), and the Youth Talent Promotion Project of the Xi'an Association for Science and Technology (095920211334).

References

[1] G. Cui, S. Ren, L. Zhang et al., "Geothermal exploitation from hot dry rocks via recycling heat transmission fluid in a horizontal well," *Energy*, vol. 128, pp. 366–377, 2017.

[2] P. Tan, H. Pang, R. Zhang et al., "Experimental investigation into hydraulic fracture geometry and proppant migration characteristics for southeastern Sichuan deep shale reservoirs," *Journal of Petroleum Science and Engineering*, vol. 184, article 106517, 2020.

[3] Y. Xue, J. Liu, P. G. Ranjith, F. Gao, H. Xie, and J. Wang, "Changes in microstructure and mechanical properties of low-permeability coal induced by pulsating nitrogen fatigue fracturing tests," *Rock Mechanics and Rock Engineering*, vol. 55, no. 12, pp. 7469–7488, 2022.

[4] J. Chen and F. Jiang, "Designing multi-well layout for enhanced geothermal system to better exploit hot dry rock geothermal energy," *Renewable Energy*, vol. 74, pp. 37–48, 2015.

[5] P. Jiang, X. Li, R. Xu, and F. Zhang, "Heat extraction of novel underground well pattern systems for geothermal energy exploitation," *Renewable Energy*, vol. 90, pp. 83–94, 2016.

[6] K. Li, H. Bian, C. Liu, D. Zhang, and Y. Yang, "Comparison of geothermal with solar and wind power generation systems," *Renewable and Sustainable Energy Reviews*, vol. 42, pp. 1464–1474, 2015.

[7] C. Li, "Types and development prospects of geothermal resources," *Management & Strategy of Qinghai Land & Resources*, vol. 4, pp. 48–53, 2014.

[8] L. Tian, "Application and development of enhanced geothermal systems(EGS)," *China Well and Rock Salt*, vol. 52, no. 4, pp. 24–26, 2021.

[9] N. Liu, N. Li, S. Wang, G. Li, and Z. Song, "A fully coupled thermo-hydro-mechanical model for fractured rock masses in cold regions," *Cold Regions Science and Technology*, vol. 205, article 103707, 2023.

[10] X. Wang, "Feasibility study on hot dry rock assisted oil recovery technique," *Strategic Study of CAE*, vol. 13, no. 3, pp. 104–106, 2011.

[11] L. Huang, J. Liu, F. Zhang, E. Dontsov, and B. Damjanac, "Exploring the influence of rock inherent heterogeneity and grain size on hydraulic fracturing using discrete element modeling," *International Journal of Solids and Structures*, vol. 176-177, pp. 207–220, 2019.

[12] N. Liu, N. Li, G. Li, Z. Song, and S. Wang, "Method for evaluating the equivalent thermal conductivity of a freezing rock mass containing systematic fractures," *Rock Mechanics and Rock Engineering*, vol. 55, no. 12, pp. 7333–7355, 2022.

[13] Y. Xue, J. Liu, X. Liang et al., "Influence mechanism of brine-gas two-phase flow on sealing property of anisotropic caprock for hydrogen and carbon energy underground storage," *International Journal of Hydrogen Energy*, vol. 48, no. 30, pp. 11287–11302, 2023.

[14] Y. Xue, P. G. Ranjith, Y. Chen, C. Cai, F. Gao, and X. Liu, "Nonlinear mechanical characteristics and damage constitutive model of coal under CO_2 adsorption during geological sequestration," *Fuel*, vol. 331, article 125690, 2023.

[15] Z. Li, H. Xu, and C. Zhang, "Liquid nitrogen gasification fracturing technology for shale gas development," *Journal of Petroleum Science and Engineering*, vol. 138, pp. 253–256, 2016.

[16] D. Tran, A. Settari, and L. Nghiem, *Initiation and Propagation of Secondary Cracks in Thermo-Poroelastic Media*, American Rock Mechanics Association, 2012.

[17] C. Cai, G. Li, Z. Huang, and H. Chi, "A waterless fracturing treatment: liquid nitrogen fracturing and its application prospect," *SOCAR Proceedings*, vol. 3, no. 3, pp. 35–40, 2015.

[18] Y. Xue, P. G. Ranjith, F. Gao, Z. Zhang, and S. Wang, "Experimental investigations on effects of gas pressure on mechanical behaviors and failure characteristic of coals," *Journal of Rock Mechanics and Geotechnical Engineering*, vol. 15, no. 2, pp. 412–428, 2023.

[19] Z. Huang, J. Wei, and G. Li, "An experimental study of tensile and compressive strength of rocks under cryogenic nitrogen freezing," *Rock and Soil Mechanics*, vol. 37, no. 3, pp. 694–700, 2016.

[20] P. Tan, Y. Jin, and H. Pang, "Hydraulic fracture vertical propagation behavior in transversely isotropic layered shale formation with transition zone using XFEM-based CZM method," *Engineering Fracture Mechanics*, vol. 248, article 107707, 2021.

[21] Y. Xue, S. Liu, J. Chai et al., "Effect of water-cooling shock on fracture initiation and morphology of high-temperature granite: application of hydraulic fracturing to enhanced geothermal systems," *Applied Energy*, vol. 337, article 120858, 2023.

[22] B. McDaniel, S. R. Grundmann, W. D. Kendrick, D. R. Wilson, and S. W. Jordan, "Field applications of cryogenic nitrogen as a hydraulic fracturing fluid," in *SPE Annual Technical Conference and Exhibition*, San Antonio, Texas, 1997.

[23] H. Wang, X. Fu, K. Jian, T. Li, and P. Luo, "Changes in coal pore structure and permeability during N_2 injection," *Journal of Natural Gas Science and Engineering*, vol. 27, pp. 1234–1241, 2015.

[24] M. Cha, X. Yin, T. Kneafsey et al., "Cryogenic fracturing for reservoir stimulation - laboratory studies," *Journal of Petroleum Science and Engineering*, vol. 124, pp. 436–450, 2014.

[25] C. Zhang, W. Li, and X. Wang, "Research of fracturing mechanism of coal subjected to liquid nitrogen cooling," *Journal of Hebei University of Science & Technology*, vol. 36, no. 4, pp. 425–430, 2015.

[26] S. R. Ren, Z. K. Fan, L. Zhang, Y. Yang, J. Luo, and H. Che, "Mechanisms and experimental study of thermal-shock effect on coal-rock using liquid nitrogen," *Chinese Journal of Rock Mechanics and Engineering*, vol. 32, no. suppplement2, pp. 3790–3794, 2013.

[27] Q. Wang, D. Zhao, and Z. Feng, "Evaluation of boron-doped-microcrystalline/nanocrystalline diamond composite coatings

in drilling of CFRP," *Coal Science and Technology*, vol. 330, no. 4, pp. 149–162, 2017.

[28] M. B. Dusseault, "Stress changes in thermal operations," in *SPE International Thermal Operations Symposium*, Bakersfield, California, 1993.

[29] T. K. Perkins and J. A. Gonzalez, "The effect of thermoelastic stresses on injection well fracturing," *Society of Petroleum Engineers Journal*, vol. 25, no. 1, pp. 78–88, 1985.

[30] X. Wu, Z. Huang, R. Li et al., "Investigation on the damage of high-temperature shale subjected to liquid nitrogen cooling," *Journal of Natural Gas Science and Engineering*, vol. 57, pp. 284–294, 2018.

[31] X. Wu, Z. Huang, H. Song et al., "Variations of physical and mechanical properties of heated granite after rapid cooling with liquid nitrogen," *Rock Mechanics and Rock Engineering*, vol. 52, no. 7, pp. 2123–2139, 2019.

[32] P. Hou, Y. Xue, F. Gao et al., "Effect of liquid nitrogen cooling on mechanical characteristics and fracture morphology of layer coal under Brazilian splitting test," *International Journal of Rock Mechanics and Mining Sciences*, vol. 151, article 105026, 2022.

[33] M. Du, F. Gao, C. Cai, S. Su, and Z. Wang, "Experimental study on the damage and cracking characteristics of bedded coal subjected to liquid nitrogen cooling," *Rock Mechanics and Rock Engineering*, vol. 54, no. 11, pp. 5731–5744, 2021.

[34] S. Su, P. Hou, F. Gao, X. Liang, R. Ding, and C. Cai, "Changes in mechanical properties and fracture behaviors of heated marble subjected to liquid nitrogen cooling," *Engineering Fracture Mechanics*, vol. 261, article 108256, 2022.

[35] B. Amadei, J. D. Rogers, and R. E. Goodman, "Elastic constants and tensile strength of anisotropic rocks," in *5th ISRM Congress*, Melbourne, Australia, 1983.

[36] I. L. Lim, I. W. Johnston, and S. K. Choi, "Stress intensity factors for semi-circular specimens under three-point bending," *Engineering Fracture Mechanics*, vol. 44, no. 3, pp. 363–382, 1993.

[37] M. R. Ayatollahi and M. R. M. Aliha, "Wide range data for crack tip parameters in two disc-type specimens under mixed mode loading," *Computational Materials Science*, vol. 38, no. 4, pp. 660–670, 2007.

[38] T. Teng, F. Gao, Z. Zhang, and Y. Gao, "Analysis of energy evolution on gas saturated raw coal under triaxial compression," *Journal of China University of Mining and Technology*, vol. 45, no. 4, pp. 663–669, 2016.

[39] J. Liu, Y. Xue, Y. Fu, K. Yao, and J. Liu, "Numerical investigation on microwave-thermal recovery of shale gas based on a fully coupled electromagnetic, heat transfer, and multiphase flow model," *Energy*, vol. 263, article 126090, 2023.